

Spectral Properties of High Contrast Band-Gap Materials and Operators on Graphs

Peter Kuchment and Leonid A. Kunyansky

CONTENTS

1. Introduction
 2. A Mathematical Framework of the Problem
 3. The Computational Algorithm
 4. Numerical Results
 5. Analytic Discussion of the Results
 6. Comparing 2D and Higher-Dimensional Cases
 7. Conclusions and Open Problems
- Acknowledgments
References

The theory of classical waves in periodic high contrast photonic and acoustic media leads to the spectral problem

$$-\Delta u = \lambda \varepsilon u,$$

where the dielectric constant $\varepsilon(x)$ is a periodic function which assumes a large value ε near a periodic graph Σ in \mathbb{R}^2 and is equal to 1 otherwise. Existence and locations of spectral gaps are of primary interest. The high contrast asymptotics naturally leads to pseudodifferential operators of the Dirichlet-to-Neumann type on graphs and on more general structures. Spectra of these operators are studied numerically and analytically. New spectral effects are discovered, among them the “almost discreteness” of the spectrum for a disconnected graph and the existence of “almost localized” waves in some connected purely periodic structures.

1. INTRODUCTION

Photonic crystals, or photonic band-gap structures, are artificially created low-loss periodic dielectric materials, whose characteristic property is the existence of *stop bands* or *gaps* in the frequency spectrum of electromagnetic waves. If the wave frequency falls in a gap, such a wave cannot propagate in the medium. The gaps arise as a result of multiple scattering and interference of waves. Acoustic analogs of such media can be also considered. Periodicity of the medium is the natural environment for spectral gaps, due to the well known band-gap structure of spectra of periodic differential operators [Ashcroft and Mermin 1976; Eastham 1973; Kuchment 1982; 1993; Reed and Simon 1978]. Due to a rich variety of expected important applications, the quest for creation of photonic crystals is very active now. One can find information about this area of research in [Bowden et al. 1993; Joannopoulos et al. 1995; John 1991; Leung and Liu 1990; Soukoulis 1993; Villaneuve and Piché 1994; Zhang and Sathpathy 1990]. The questions of possibility of cre-

Work of both authors was partially supported by the NSF Grant DMS-9610444 and by a DEPSCoR Grant administered through the ARO. The first author was also partially supported by an NSF EPSCoR Grant. The content of this article does not necessarily reflect the position or the policy of the federal government.

ating band gaps, of relations between the geometric and physical parameters of a medium and its spectral structure, and of reliable numerical analysis are among the most important ones. Until recently, the research had mainly concentrated on experimental and numerical study of photonic band-gap structures. Mathematical analysis of the problem was started in [Figotin 1994; Figotin and Godin 1997; Figotin and Kuchment 1996a; 1995; 1998a; 1996b; 1998b]. In particular, it was rigorously proved that band gaps can be created in 2D square structures. An asymptotic analysis of the problem was undertaken for the case when the volume fraction of the optically dense portion of the dielectric tends to zero, while its “mass” (the product of the volume fraction by the dielectric constant) tends to infinity. It was discovered that there are two parts of the spectrum, having different asymptotic behavior. Namely, one type of eigenmodes prefers to stay inside the air bubbles. The corresponding spectrum shrinks to the spectrum of the Dirichlet or Neumann Laplacian (depending on polarization) on the air bubble, which leads to the opening of wide gaps. Another type of modes propagate almost exclusively inside the thin optically dense dielectric walls. The corresponding spectrum consists of very narrow spectral bands separated by narrow gaps. It was shown in [Figotin and Kuchment 1998b] that the operator responsible for this “bad” type of spectrum is a pseudodifferential “Dirichlet-to-Neumann” operator on a graph. A generalization of this result will be provided in [Figotin and Kuchment – to appear]. It is interesting to notice that differential operators on graphs (or on surface structures in higher dimensions) also arise as asymptotic models of mesoscopic physics in microelectronics, superconductivity, chemistry, and other areas; see [Exner and Seba 1989; 1995; Freidlin and Wentzell 1993; Carlson 1997; 1998; 1999; Rubinstein and Schatzman 1998; Schatzman 1996], and references therein).

In this paper we undertake a numerical and analytic study of the pseudodifferential operators on graphs mentioned above. It turns out that spectra of such operators display interesting and unexpected features. We provide some discussion of these effects. This study naturally extends the analysis of [Figotin and Kuchment 1998b].

We see the role of asymptotic models as follows. First, they clarify many spectral properties that are obscured in the non-asymptotic case. Secondly, they

are usually much easier to treat numerically, due to the reduction in dimension that occurs in the asymptotic limit. Besides, the eigenmodes obtained for an asymptotic model can be used as a basis for Rayleigh–Ritz type numerical methods for the complete model [Figotin and Godin 1997; Ponomarev 1999]. In many cases asymptotic models take into account singularities of the problem that impede its direct study by, for instance, Fourier type methods. Finally, they supply information about possible spectral effects and behavior of eigenmodes, thus providing a natural basis for subsequent consideration of the complete non-asymptotic model.

In this paper we outline numerical results about spectra and analyze the spectral effects discovered. As explained later on, only the most “troublesome” type of eigenmodes and corresponding spectra is discussed, namely the waves that are mostly localized inside of the optically dense dielectric region of the medium.

We briefly describe the contents of the paper. Section 2 is devoted to the description of the mathematical model of electromagnetic waves in photonic crystals. Section 3 contains a description of the computational algorithm used. We provide numerical results in Section 4 and formulate related analytic results in Section 5. Section 6 is devoted to discussion of differences between the 2D and higher-dimensional cases. Finally, Section 7 contains conclusions and some open problems.

2. A MATHEMATICAL FRAMEWORK OF THE PROBLEM

The main object of our consideration is a periodic dielectric or acoustic medium occupying \mathbb{R}^3 or \mathbb{R}^2 . Properties of the medium can be described by a scalar function $\varepsilon(\mathbf{x})$ on \mathbb{R}^3 or \mathbb{R}^2 , which is the dielectric constant for dielectric media, or the compressibility for elastic media. We call $\varepsilon(\mathbf{x})$ the dielectric constant. Suppose that the medium consists of two types of components and hence the function $\varepsilon(\mathbf{x})$ assumes two values, say 1 and $\varepsilon > 1$ (due to natural rescaling properties, only the ratio of these two values matters, so our assumption does not restrict generality; see [Joannopoulos et al. 1995]). One can imagine that the component of the medium with $\varepsilon(\mathbf{x}) = 1$ is filled with air and the one with $\varepsilon(\mathbf{x}) = \varepsilon > 1$ is filled with some optically dense dielectric material. The object of our study is a high contrast medium, where the dense component

occupies thin walls of thickness $\delta \ll 1$ (and hence of volume fraction of order $\delta \ll 1$) and the total “optical mass” $\varepsilon\delta$ of the dense component per unit volume does not approach zero. In particular, $\varepsilon\delta$ can be very large.

2A. The Maxwell Operator

Electromagnetic wave propagation in our dielectric medium can be described by the standard Maxwell equations

$$\nabla \cdot \mathbf{D} = 0, \quad \nabla \times \mathbf{E} = -\frac{1}{c} \frac{\partial \mathbf{B}}{\partial t}, \quad \mathbf{D} = \varepsilon \mathbf{E}, \quad (2-1)$$

and

$$\nabla \cdot \mathbf{B} = 0, \quad \nabla \times \mathbf{H} = \frac{1}{c} \frac{\partial \mathbf{D}}{\partial t}, \quad \mathbf{B} = \mu \mathbf{H}, \quad (2-2)$$

where \mathbf{E} is the electric field, \mathbf{D} is the electric induction, \mathbf{H} and \mathbf{B} are respectively the magnetic field and magnetic induction, and c is the velocity of light. We shall assume that $\mu \equiv 1$ (this condition holds for most dielectric materials of interest). The dielectric constant ε is assumed to be position-dependent, that is, $\varepsilon = \varepsilon(\mathbf{x}) \geq 1$. Assuming that the wave is monochromatic with frequency ω , one can reduce this system to one of two equivalent models

$$\nabla \times (\varepsilon(\mathbf{x})^{-1} \nabla \times \mathbf{H}(\mathbf{x})) = \left(\frac{\omega}{c}\right)^2 \mathbf{H}(\mathbf{x}) \quad (2-3)$$

or

$$\varepsilon(\mathbf{x})^{-1} \nabla \times (\nabla \times \mathbf{E}(\mathbf{x})) = \left(\frac{\omega}{c}\right)^2 \mathbf{E}(\mathbf{x}) \quad (2-4)$$

under the additional conditions of zero divergence $\nabla \cdot \mathbf{H} = \mathbf{0}$ and $\nabla \cdot \varepsilon \mathbf{E} = \mathbf{0}$, respectively. Hence, we have to study the spectral problem for one of the operators

$$\nabla \times \varepsilon(\mathbf{x})^{-1} \nabla \times \quad (2-5)$$

or

$$\varepsilon(\mathbf{x})^{-1} \nabla \times \nabla \times, \quad (2-6)$$

with appropriate zero divergence conditions, where $(\omega/c)^2$ plays the role of the spectral parameter. It is well known — see, for instance, [Joannopoulos et al. 1995] — that these two problems are unitarily equivalent, and hence have the same spectra. The main question of interest is how the spectrum is related to the geometry and dielectric constant of our periodic medium — in particular, whether it is possible to create spectral gaps at desired places of the frequency spectrum.

2B. Two-Dimensional Photonic Crystals

In this paper (apart from Section 6) we deal mostly with two-dimensional media; see also [Bowden et al. 1993; Joannopoulos et al. 1995; Maradudin and McGurn 1993; McCall et al. 1991; Meade et al. 1992; Plihal and Maradudin 1991; Sigalas et al. 1993; Soukoulis 1993; Villeneuve and Piché 1991] for the study of 2D photonic band gap structures. Our study will take place in the real plane \mathbb{R}^2 , which represents our 2D medium, that is, a cross-section of a 2D photonic crystal. For two-dimensional photonic crystals, when $\varepsilon(x)$ does not depend on the vertical variable, and for the waves propagating in the crystal’s plane \mathbb{R}^2 , the Maxwell operator can be represented as the direct sum of two scalar operators. These operators correspond to the so called *TE* and *TM* polarizations of waves. In the *TE* polarization the electric field is directed along the plane of periodicity, while in *TM* polarization it is the magnetic that satisfies this property. This splitting leads to a decomposition of the spectrum into two subspectra. The corresponding scalar eigenvalue problems in $L_2(\mathbb{R}^2)$ are

$$-\nabla \cdot \varepsilon^{-1} \nabla u = \lambda u \quad (2-7)$$

and

$$-\Delta u = \lambda \varepsilon u. \quad (2-8)$$

The same scalar problems describe propagation of acoustic waves in elastic media, so considering them in 3D also makes sense. The case of such periodic 2D dielectric or acoustic media, when the “air” domains are squares and the periods form a square lattice, was studied in [Figotin and Kuchment 1996a; 1995; 1998a; 1996b] under the condition that

$$\varepsilon\delta \gg 1, \quad \varepsilon\delta^2 \ll 1. \quad (2-9)$$

It was shown that the asymptotic behavior under condition (2-9) is different for the spectra of problems (2-7) and (2-8). Namely, the spectrum of problem (2-7) shrinks to the (discrete) spectrum of the Dirichlet Laplacian on the fundamental domain of the group of periods. In the case of square geometry this is just the unit cube, and hence the Dirichlet spectrum consists of numbers $\pi^2(n^2 + m^2)$, where m and n are integers. In particular, large gaps can be opened in this spectrum. We shall call it the “good” spectrum. The Floquet–Bloch eigenmodes

(see [Eastham 1973; Kuchment 1993; Reed and Simon 1978] and Section 3 of this paper) are mainly concentrated inside the air bubbles, where $\varepsilon = 1$.

A very different asymptotic behavior is demonstrated by the spectrum of problem (2–8), which corresponds to *TM* polarized waves. In this case there are two types of eigenmodes. The first corresponds to the waves that mostly stay inside the air bubbles. The corresponding spectrum shrinks asymptotically, under (2–9), to the (discrete) spectrum of the Neumann Laplacian on the fundamental domain (the unit cube in this case). However, there is another, “bad” type of eigenmodes that propagate mainly inside the thin areas where ε is large. The corresponding spectrum in the limits (2–9) asymptotically consists of narrow bands alternating with gaps, both of width $(\varepsilon\delta)^{-1}$. Thus spectral gaps do arise, but they become very small. We can call this spectrum the “bad” spectrum, since it creates obstacles to opening large gaps. This description implied the first analytical proof of the possibility of creating band gaps in photonic crystals. Besides, the asymptotic behavior of the spectrum in the case of square plane geometry was well understood. Moreover, understanding the nature of the eigenmodes gave some insights into what kind of problems one can face computing these spectra numerically. Namely, very singular behavior of the eigenmodes of the “bad” spectrum suggests that if one tries to use Fourier type methods without taking into account the singularities, some crucial spectral information can be lost. This remark is in agreement with the effects discovered numerically in [Villaneuve and Piché 1994], where the numerically computed spectra of the two equivalent problems (2–5) and (2–6) were different.

However, many important issues were not considered in [Figotin and Kuchment 1996a; 1995; 1998a; 1996b]. The main one is that only the square geometry was treated. This was the natural consequence of the adopted approach of separation of variables. Practically no other geometry can be treated this way. A new approach was suggested in [Figotin and Kuchment 1998b], where an asymptotic model was obtained under much less restrictive asymptotic conditions than in the earlier papers, and arbitrary geometries were treated. We describe briefly the main result of this more recent paper, since our investigation will start from that point. Its results hold in any dimension, but we will treat here mostly the 2D case.

Consider the Euclidean plane \mathbb{R}^2 . Suppose that \mathbb{R}^2 is tessellated (tiled) with polygons Ω_p and that this tessellation is periodic with respect to a discrete group Γ of motions of the plane. We assume that the fundamental domain of Γ is compact. In all our examples below Γ will consist of integer linear combinations of two vectors a and b , usually parallel to the coordinate axes. Denote by Σ the union of all boundaries of the polygons Ω_p ; this is a Γ -periodic graph in \mathbb{R}^2 (Figure 1, top). We consider here not combinatorial graphs, that is, collections of vertices with assigned connections, but rather topological graphs as one-dimensional “varieties” in the plane consisting of segments that represent the edges of the graph. Choose a small number $\delta > 0$ and consider the δ -neighborhood Σ_δ of Σ . Define $U_\delta = \mathbb{R}^2 \setminus \Sigma_\delta$. Now imagine that U_δ , which is a locally finite union of bounded domains, is filled with air (i.e., $\varepsilon = 1$ there) and Σ_δ is filled with an optically dense dielectric (i.e., $\varepsilon > 1$ there). In this way we obtain a 2D photonic crystal defined by the dielectric function $\varepsilon(x)$ (Figure 1, bottom).

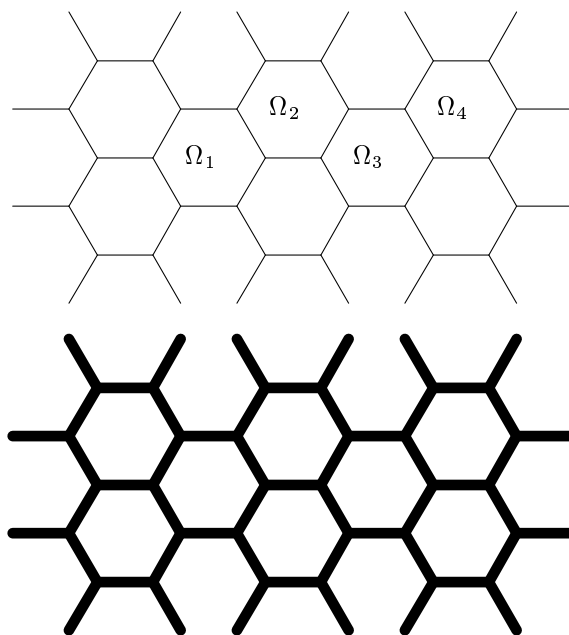


FIGURE 1. A graph Σ (top) and the corresponding 2D photonic crystal.

In particular, we can consider problems (2–7) and (2–8) in this setting. We will be concerned here only with problem (2–8), which is responsible for the “bad” spectrum.

Now consider the asymptotic assumptions

$$\delta \rightarrow 0, \quad \varepsilon\delta \rightarrow W^{-1} \in (0, \infty]. \quad (2-10)$$

Notice that these assumptions about the parameters of the medium are significantly weaker (especially when $W \neq 0$) than (2–9). It was shown in [Fiotin and Kuchment 1998b] that in this limit, after rescaling λ to a new spectral parameter D by setting

$$\lambda = (\varepsilon\delta)^{-1}D,$$

any finite part of the spectrum (in terms of values of D) of problem (2–8) tends to the corresponding part of the spectrum of the problem

$$-\Delta u = D(\delta_\Sigma + W)u. \quad (2-11)$$

Here δ_Σ is the δ -function on the graph Σ ; that is, for any smooth compactly supported function $\varphi(x)$ on \mathbb{R}^2 the value of the distribution δ_Σ on φ is defined by

$$\langle \delta_\Sigma, \varphi \rangle = \int_\Sigma \varphi(x) d\sigma,$$

where $d\sigma$ is the arc length measure on Σ . In particular, when $W = 0$, i.e., when the “mass” $\delta\varepsilon$ of the dielectric part of a fixed volume of the medium tends to infinity, the limit problem is

$$-\Delta u = D\delta_\Sigma u. \quad (2-12)$$

2C. The Dirichlet-to-Neumann Operator

The spectrum of problem (2–12) can be described in terms of the spectrum of a Dirichlet-to-Neumann type pseudodifferential operator on Σ . (Such operators are currently very popular due to their relation to important inverse conductivity problems: see [Sylvester and Uhlmann 1988].) This operator is defined as follows. Let φ be a function (from an appropriate functional class) on the surface Σ . Using φ as the boundary data, we solve in each of the polygons Ω_p the Dirichlet boundary value problem for the equation $-\Delta u = 0$. The resulting functions in different polygons match on the common boundaries, but their normal derivatives do not match. The jump of the normal derivative across Σ gives another function ψ on Σ . In this way we determine the “Dirichlet-to-Neumann” operator $N : \varphi \rightarrow \psi$. Now the spectrum of problem (2–12) coincides with the spectrum of the operator N .

2D. Statement of the Problem

The main goal of this paper is to study the spectral problem (2–12) for different geometries of the graph Σ . We are interested in existence of gaps, their sizes and locations, dispersion relations, etc. The case

when the graph Σ is not connected is also considered. Some interesting new effects are discovered, namely periodicity of the spectrum, the “almost discreteness” of the spectra of disconnected structures, and the existence of strange spikes in the density of states for some connected periodic structures. We also provide some initial analytic explanations for these effects. Problems (2–11) and (2–8), as well as the complete 3D case, will be considered elsewhere.

3. THE COMPUTATIONAL ALGORITHM

In this section we describe the algorithm that was used for numerical study of the spectral problem (2–12). We assume that the medium under consideration is periodic with periods p_1 and p_2 in the directions of the variable axes x_1 and x_2 , respectively. In other words, the group of periods is

$$\Gamma = \{(p_1 n_1, p_2 n_2) : n_1, n_2 \in \mathbb{Z}\}.$$

The first step of the algorithm is to rescale the problem in such a way that both periods equal 1. So, from now on we will assume for simplicity that this is the case.

Each elementary cell of the medium contains a translated copy of some polygonal structure S consisting of a finite number of segments S_j :

$$S = \bigcup_j S_j.$$

The whole graph Σ is obtained by replication S by the group of periods. Each segment S_j is determined by its length l_j , the coordinates of one endpoint \mathbf{b}_j , and the unit vector \mathbf{s}_j directed along the segment. The spectral problem in $L_2(\mathbb{R}^2)$ that we need to solve is

$$-\Delta u = D\delta_\Sigma u.$$

Due to the periodicity of δ_Σ , this problem can be treated according to the standard Floquet theory [Eastham 1973; Kuchment 1982; 1993; Reed and Simon 1978], which says that the spectrum can be represented as the union over $\mathbf{k} = (k_1, k_2)$ of (discrete) spectra of the following Floquet–Bloch boundary value problems on the fundamental cell $\{0 \leq x_m \leq 1 : m = 1, 2\}$:

$$-\Delta u(\mathbf{x}) = D \left(\sum \delta_{S_j}(\mathbf{x}) \right) u(\mathbf{x}), \quad (3-1)$$

with

$$\begin{aligned} u(1, x_2) &= e^{ik_1} u(0, x_2), & u_{x_1}(1, x_2) &= e^{ik_1} u_{x_1}(0, x_2), \\ u(x_1, 1) &= e^{ik_2} u(x_1, 0), & u_{x_2}(x_1, 1) &= e^{ik_2} u_{x_2}(x_1, 0). \end{aligned}$$

Here $\delta_{S_j}(\mathbf{x})$ is the delta-function of the segment S_j , i.e.,

$$\langle \delta_{S_j}, \varphi \rangle = \int_{S_j} \varphi(x) d\sigma,$$

and the union of spectra is taken over the set of *quasimomenta* $\mathbf{k} = (k_1, k_2)$ such that

$$0 \leq k_m \leq 2\pi,$$

i.e., the quasi-momentum $\mathbf{k} = (k_1, k_2)$ belongs to the Brillouin zone $B = [0, 2\pi] \times [0, 2\pi]$.

The substitution $\varphi(\mathbf{x}) = e^{i\mathbf{k} \cdot \mathbf{x}} u(\mathbf{x})$ leads to the equation

$$\begin{aligned} A_{\mathbf{k}} \varphi(\mathbf{x}) &\equiv - \sum_{m=1,2} (\partial_m - ik_m)^2 \varphi(\mathbf{x}) \\ &= D \left(\sum_j \delta_{S_j}(\mathbf{x}) \right) \varphi(\mathbf{x}), \end{aligned}$$

with periodic boundary conditions

$$\begin{aligned} \varphi(1, x_2) &= \varphi(0, x_2), \quad \varphi_{x_1}(1, x_2) = \varphi_{x_1}(0, x_2), \\ \varphi(x_1, 1) &= \varphi(x_1, 0), \quad \varphi_{x_2}(x_1, 1) = \varphi_{x_2}(x_1, 0). \end{aligned}$$

Here $A_{\mathbf{k}}$ can be considered as an operator on the torus $\mathbb{T}^2 = \mathbb{R}^2 / \mathbb{Z}^2$. Fourier expansion

$$\varphi(\mathbf{x}) = \sum_{\mathbf{n} \in \mathbb{Z}^2} \Phi_{\mathbf{n}} e^{2\pi i \mathbf{x} \cdot \mathbf{n}}$$

reduces $A_{\mathbf{k}}$ to multiplication by $(2\pi\mathbf{n} + \mathbf{k})^2$. For any quasi-momentum \mathbf{k} in the Brillouin zone, except zero, this operator has a Green's function. The value $\mathbf{k} = 0$ can be avoided, since the spectrum of the problem can be described as the closure of the union of spectra for any dense subset of values of quasimomenta in the Brillouin zone; see, for instance, the proof of a similar statement in [Figotin and Kuchment 1996b]. Instead of the value $\mathbf{k} = 0$ some values with small $|\mathbf{k}|$ were chosen. (A different type of computation was also conducted that does include $\mathbf{k} = 0$. It shows that no significant error was made by avoiding this value.) Take $\mathbf{k} \in B$, $\mathbf{k} \neq 0$, and let $G_{\mathbf{k}}(x - y)$ be the corresponding Green's function. Our spectral problem can be rewritten as

$$\frac{1}{D} \varphi(\mathbf{x}) = \int_{\Omega} G_{\mathbf{k}}(\mathbf{x} - \mathbf{y}) \left(\sum_j \delta_{S_j}(\mathbf{y}) \right) \varphi(\mathbf{y}) d\mathbf{y}.$$

Denote by $\psi_j(t)$ the restriction of the function $\varphi(\mathbf{x})$ to the segment S_j :

$$\psi_j(t) = \varphi(\mathbf{b}_j + t\mathbf{s}_j), \quad \text{for } 0 \leq t \leq l_j.$$

Then the problem can be reformulated using one-dimensional convolution

$$\lambda \psi_m(t) = \sum_j \int_0^{l_j} G(\mathbf{b}_m + t\mathbf{s}_m - (\mathbf{b}_j + \tau\mathbf{s}_j)) \psi_j(\tau) d\tau,$$

where $\lambda = 1/D$. In order to truncate it to a standard matrix eigenvalue problem, we sample the functions ψ_j , setting

$$\psi_j^r = \psi_j(t_r), \quad \text{where } t_r = (r - 1)\Delta t,$$

and approximate each $\psi_j(t)$ using an appropriate point-spread function $B(t)$:

$$\psi_j(t) \approx \sum_r \psi_j^r B(t - t_r).$$

Then we obtain

$$\lambda \psi_m^p = \sum_{j,r} \psi_j^r \int G_{\mathbf{k}}(\mathbf{b}_m + t_p\mathbf{s}_m - (\mathbf{b}_j + \tau\mathbf{s}_j)) B(\tau - t_r) d\tau,$$

or

$$\begin{aligned} \lambda \psi_m^p &= \sum_{j,r} \psi_j^r \int G_{\mathbf{k}}(\mathbf{b}_m + t_p\mathbf{s}_m - (\mathbf{b}_j + t_r\mathbf{s}_j) - \tau\mathbf{s}_j) B(\tau) d\tau. \end{aligned}$$

Now the problem is reduced to the eigenvalue problem for a matrix $\mathbf{G} = \{g_{m,j}^{p,r}\}$ with entries

$$g_{m,j}^{p,r} = g_j(\mathbf{b}_m + t_p\mathbf{s}_m - (\mathbf{b}_j + t_r\mathbf{s}_j)), \quad (3-2)$$

where the functions $g_j(\mathbf{x})$ are defined by

$$g_j(\mathbf{x}) = \int G_{\mathbf{k}}(\mathbf{x} - \tau\mathbf{s}_j) B(\tau) d\tau.$$

Denote by $\beta_j(\mathbf{x})$ the following extension of the function $B(\tau)$ from segment S_j to the whole 2D domain:

$$\beta_j(\mathbf{x}) = \delta(\mathbf{x} \cdot \mathbf{s}_j^\perp) B(\mathbf{x} \cdot \mathbf{s}_j),$$

where $\mathbf{s}_j^\perp \cdot \mathbf{s}_j = 0$. Then g_j can be understood as the 2D convolution of $G_{\mathbf{k}}(\mathbf{x})$ with $\beta_j(\mathbf{x})$:

$$g_j(\mathbf{x}) = \int G_{\mathbf{k}}(\mathbf{x} - \xi) \beta_j(\xi) d\xi. \quad (3-3)$$

In order to construct the matrix \mathbf{G} , we need to compute the functions $g_j(\mathbf{x})$. The Fourier coefficients $\Xi_{j,\mathbf{n}}$ of $\beta_j(\mathbf{x})$ are

$$\Xi_{j,\mathbf{n}} = \hat{B}(\mathbf{n} \cdot \mathbf{s}_j),$$

where $\hat{B}(\rho)$ is the 1D Fourier transform of $B(t)$. Functions $g_j(\mathbf{x})$ can be calculated for a fixed quasi-momentum $\mathbf{k} \in B$, $\mathbf{k} \neq 0$, as sums of Fourier series:

$$g_j(\mathbf{x}) = \sum_{\mathbf{n} \in \mathbb{Z}^2} e^{2\pi i \mathbf{x} \cdot \mathbf{n}} \hat{B}(\mathbf{n} \cdot \mathbf{s}_j) (2\pi\mathbf{n} + \mathbf{k})^{-2}. \quad (3-4)$$

Approximate calculation of $g_j(\mathbf{x})$ and hence of the matrix G can be now implemented according to a

truncated version of the formula (3–4). The use of FFT makes the computation efficient. However, precise calculation, especially of the values $g_j(0)$, which stand on the main diagonal of the matrix \mathbf{G} , is necessary to obtain a satisfactory result. Here the correct choice of function $B(t)$ is crucial. If, for instance, $B(t)$ is the δ -function ($\hat{B}(\rho) \equiv 1$), the series (3–4) diverges. We obtained the best results with the following choice of $B(t)$. Let $\rho_{\max} = 1/(2\Delta t)$ be the Nyquist frequency for the sampling step Δt . We define the Fourier transform of $B(t)$ as the once continuously differentiable spline $\hat{B}(\rho)$, where $\hat{B}(\rho) = 1$ when $|\rho| \leq 0.9\rho_{\max}$, $\hat{B}(\rho) = 0$ when $|\rho| \geq 1.1\rho_{\max}$, and $\hat{B}(\rho)$ is a cubic polynomial when $0.9\rho_{\max} \leq |\rho| \leq 1.1\rho_{\max}$. Values of $g_j(\mathbf{x})$ are computed using a truncated version of (3–4) (for $|n_1|, |n_2| \leq N$) on a square grid in the unit square. In order to increase accuracy of calculation of $g_j(0)$, we correct these values adding an estimate $\delta g_j(0)$ of the truncation error. We estimate the truncation error, computing numerically the integral

$$\delta g_j(0) = \int_{\mathbb{R}^2 \setminus \mathcal{X}} \hat{B}(\xi \cdot \mathbf{s}_j) (2\pi\xi + \mathbf{k})^{-2} d\xi, \quad (3-5)$$

where integration is carried out over the exterior of the square \mathcal{X} with side $2N+1$ centered at the origin. Now standard methods for numerical calculation of the spectrum can be used. We used $N = 2^9$ and $\Delta t \sim 10^{-2}$. We recall that the fundamental cell is the unit square.

In the next sections we describe our numerical results and results of some accuracy tests.

4. NUMERICAL RESULTS

4A. Square Geometry. Tests of Accuracy

In order to verify the reliability of the algorithm we calculated the spectrum for a square lattice of infinitely thin dielectric rods. This structure is generated by two perpendicular segments S_1 and S_2 in the unit square $[0, 1] \times [0, 1]$, as shown in Figure 2, top. In this case the spectrum can be found analytically by separation of variables; see [Figotin and Kuchment 1998b]. It consists of numbers D such that for some $\eta > 0$ the following system of transcendental inequalities is satisfied:

$$\left| \cos \eta - \frac{D}{2\eta} \sin \eta \right| \leq 1, \quad \left| \cosh \eta - \frac{D}{2\eta} \sinh \eta \right| \leq 1.$$

This gives us the opportunity to compare the solutions given by our numerical algorithm with those of

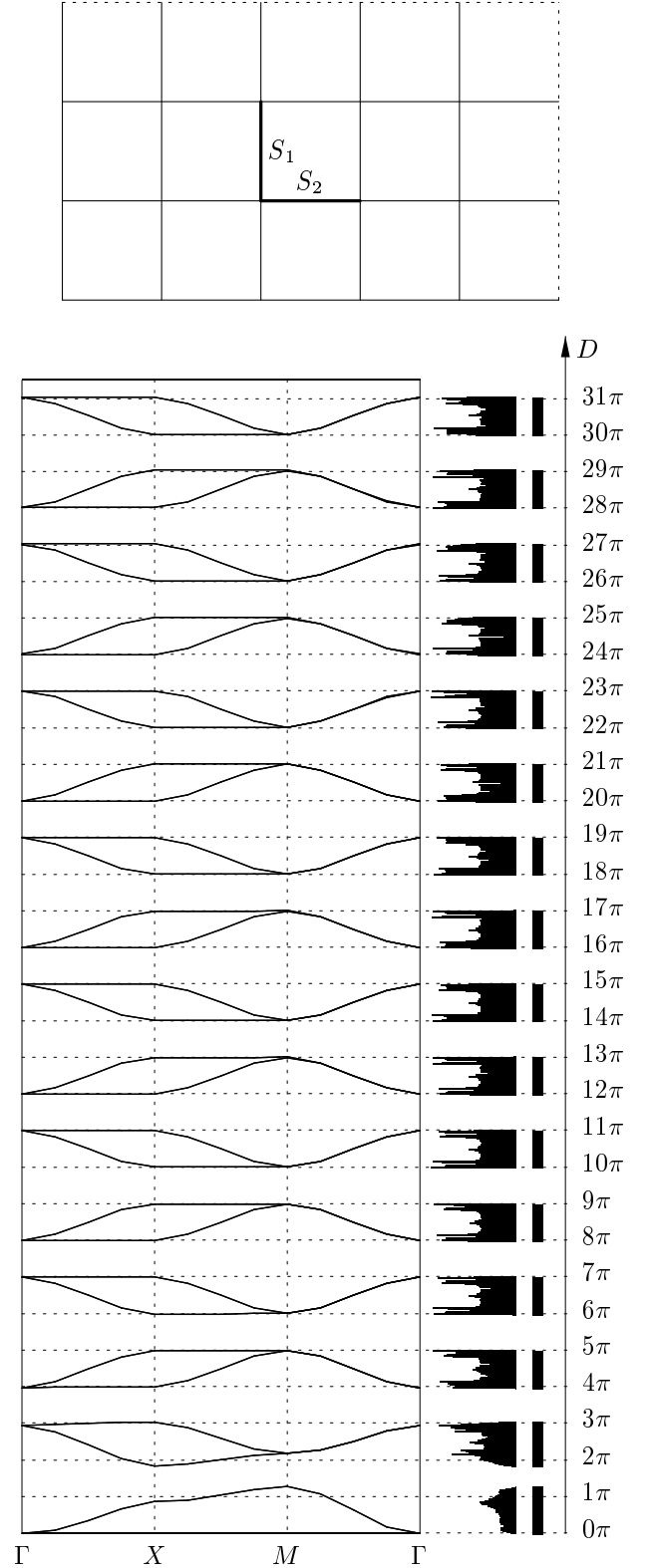


FIGURE 2. Square structure and its spectrum, as obtained by the algorithm. In this and subsequent figures, the vertical axis on the right is the spectral axis; the black vertical bars indicate the spectrum; the jagged graphs indicate the density of states; and the curves show the dispersion relations.

the transcendental system. It is known (see [Figotin and Kuchment 1996b]) that the spectrum consists of bands that converge to the segments $[2\pi n, 2\pi n + \pi]$ as D goes to infinity; the first band, corresponding to $n = 0$, is close to the segment $[0, 4]$. A direct numerical solution of the transcendental system gives the following result for the first three bands:

Band number n	Beginning	End
0	0.000	4.006
1	5.759	9.425
2	12.582	15.775

Starting with $n \geq 4$, the bands practically coincide with the intervals $[2\pi n, 2\pi n + \pi]$.

Figure 2, bottom, shows the results obtained by the algorithm presented in the previous section. In this picture the spectral axis is vertical. The first column represents the graphs of several branches of the dispersion relation $D_j(\mathbf{k})$. In order to avoid graphing surfaces, the dispersion relation is graphed only for the values of the quasimomentum \mathbf{k} on the boundary of the irreducible Brillouin zone, which is the triangle with vertices $\Gamma(0, 0)$, $X(\pi, 0)$, and $M(\pi, \pi)$. The second column contains the graph of the density of states over the spectral axis. (We recall the notion of the density of states in Section 5.) The third column shows the band-gap structure of the spectrum. The endpoints of the bands thus obtained agree with the expected values within 0.1% accuracy for at least the first sixteen bands.

Another accuracy check was performed as follows. The same geometric structure, in our case the square lattice, can be obtained by periodic replication of different sets of segments. If the algorithm were inaccurate there would be no reason for it to produce the same results for these different representations. On the other hand, if the algorithm is correct, the spectra must agree. Thus we used a structure generated by the two diagonals of the square of side $\sqrt{2}$; this structure is congruent with the original one (under a 45° rotation). Our computations in both cases lead to the same spectrum. The discrepancy for several lower bands does not exceed 0.1%. Another attempt to “trick” the algorithm was undertaken using the four halves of these two diagonals instead of the whole diagonals. The computed spectrum practically did not change. All these results show that the algorithm is reliable.

4B. Rectangular Structures

The algorithm was applied to two structures consisting of translated rectangles. The first one is generated by three segments in the unit square (Figure 3, top). The rectangular cells have ratio 2:1 between sides. The spectrum shows periodic behavior for large values of the spectral parameter D (Figure 3, bottom). For higher frequencies it appears to be the superposition of two series of bands. The first one corresponds to the case of the unit square structure. The second series is the first one dilated by a factor of 2.

The second rectangular structure consists of rectangles with side ratio $\sqrt{2} : 1$. The spectrum, shown in Figure 4, no longer shows any periodicity.

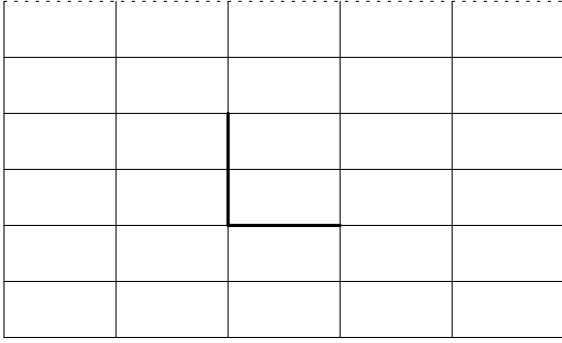
It appears that at high frequencies each of the two sides of the rectangular cell is responsible for its own series of spectral bands. This would explain the disappearance of the periodic structure of the spectrum in the case of incommensurable sides of the rectangular cell. In fact, this can be justified by a separation of variables analysis similar to the one used in [Figotin and Kuchment 1998b] and in the previous section. A system of transcendental equations can be written and easily analyzed. The corresponding analytic results agree well with the results of our numerical analysis.

“Brick” structures (with alternating rows of rectangles) show effects similar to the ones obtained in rectangular cases.

4C. Disconnected Dielectric Structures

A *disconnected structure* is one whose periodic graph Σ consists of disjoint compact pieces. We considered the cases when Σ consisted of repeated disjoint circles, disjoint segments, disjoint crosses, disjoint squares, and some other disconnected graphs. Spectra of all these disconnected dielectric structures possess an interesting property: as the band number increases, the bands become very thin, creating what is practically a “point” spectrum. Besides, several of these structures exhibit apparent asymptotic periodicity of the spectrum.

A circle structure was generated by translating a circle of radius 0.2 (Figure 5, top), approximated by a sixteen-edge inscribed polygon. This disconnected structure produces an asymptotically periodic and “almost discrete” spectrum; see Figure 5, bottom. The narrow bands of the spectrum are situated near



the numbers $2n/r$, where r is the radius of the circle; this effect will be explained in a later section. Note that $2n/r$ can be also written as $4\pi n/L$, where L is the length of the circle.

The structure generated by one segment of length $L = 0.5$ in the unit square and its spectrum are shown in Figure 6. The spectrum is asymptotically periodic, the phenomenon of “almost discreteness” is clearly visible, and the bands are located close

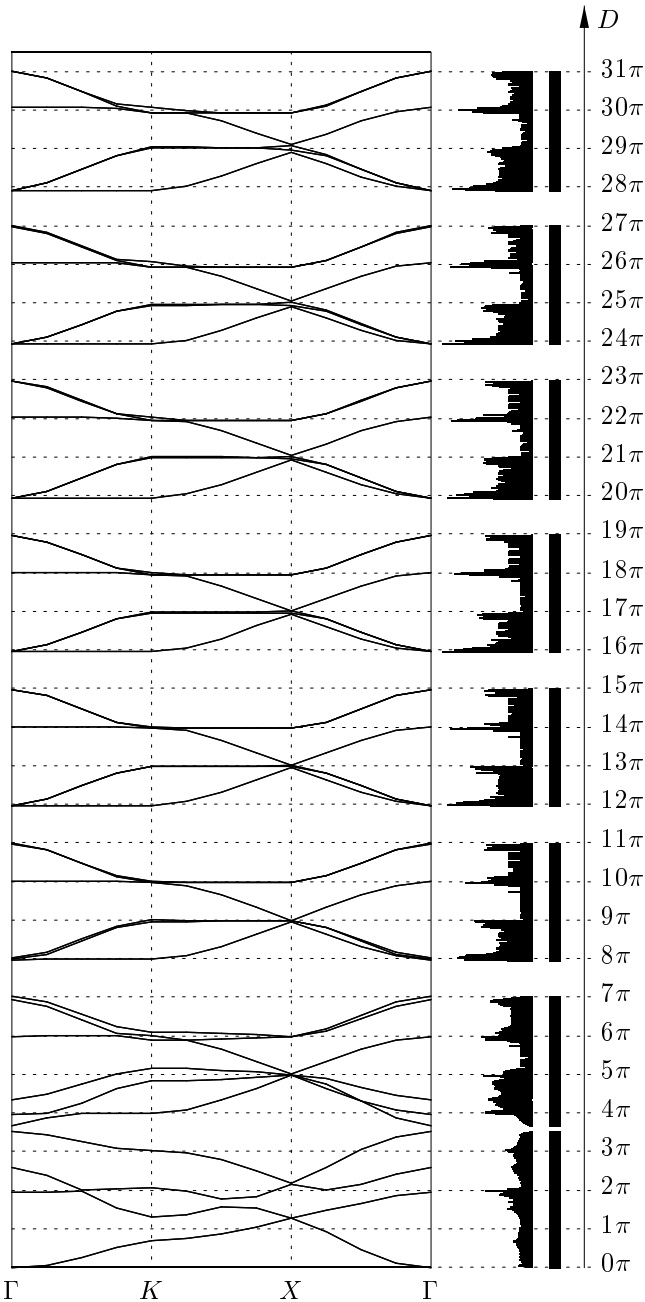


FIGURE 3. Rectangular structure with side ratio 1:2 and its spectrum.

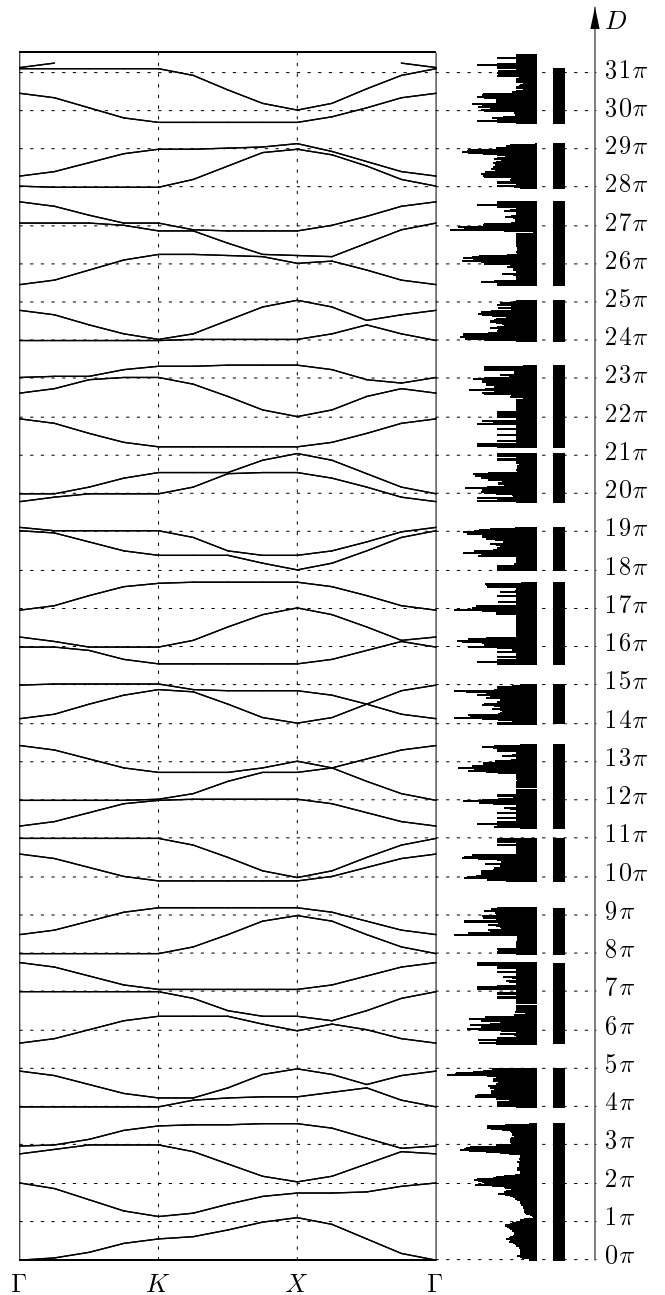


FIGURE 4. Spectrum of rectangular structure with side ratio $\sqrt{2} : 1$.

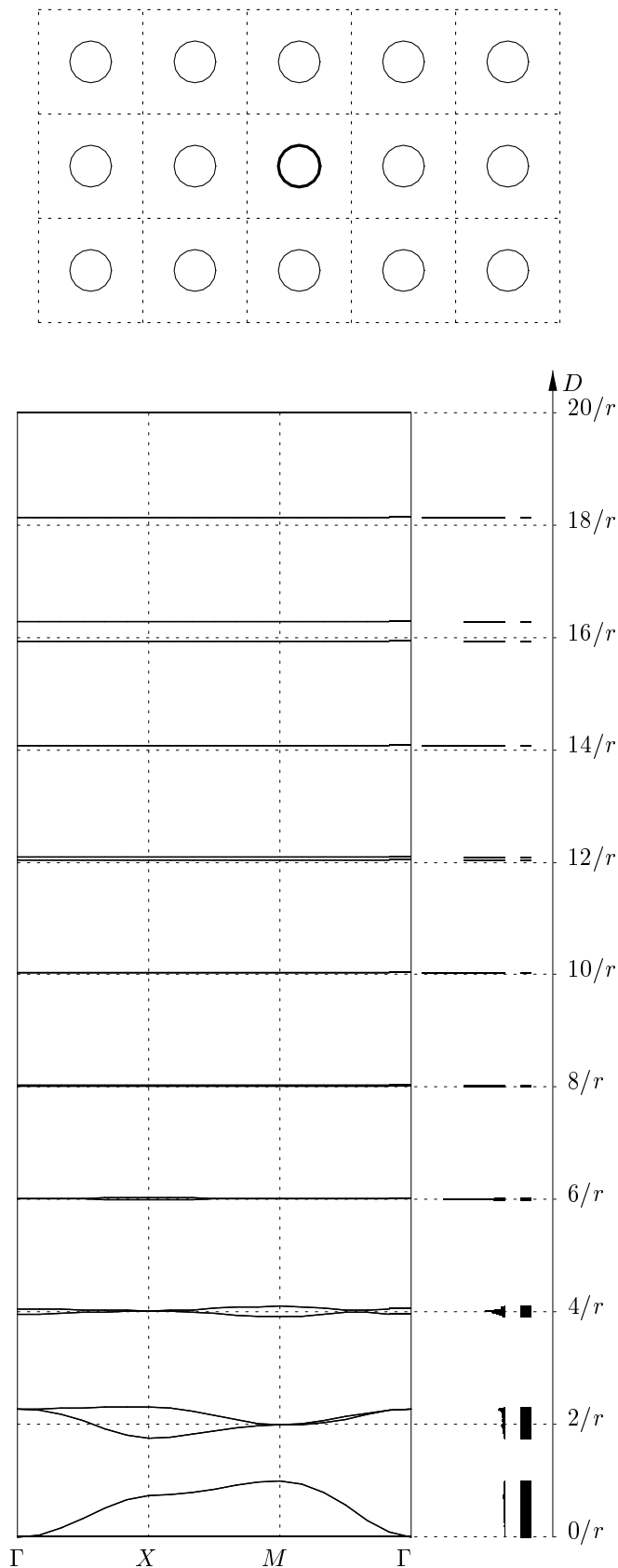


FIGURE 5. A disconnected circle structure and its spectrum. In the vertical axis, $r = 0.2$ is the radius of the circles (the squares have side 1).

to the numbers $2n\pi/L$. It looks like we have the same formula for location of bands as in the case of a circle, if we think of a segment as being double-sided (and therefore of double length). However, even with this double-sidedness trick, the agreement with the formula for the circle case is much better than for a single segment. In the case of a segment one sees an apparently regular shift from the value predicted by the formula $2n\pi/L$. We believe that this reflects the role played by the singularities (endpoints of the segment). An initial discussion will be provided in Section 5, and a more detailed investigation is planned for the next paper.

The cross structure (Figure 7, bottom) is created from the previous one by adding a second segment orthogonal to the first. Its spectrum is again asymptotically periodic and “almost discrete”. The bands located right above the frequencies $(2n + 1)2\pi/0.5$ bring to mind the odd-numbered bands of the previous structure (Figure 6).

An analogous effect was discovered in the periodic disconnected structure that is obtained by repeating a square.

It is interesting to mention the existence of an “almost point” subspectrum in some (but not all) connected dielectric structures. This topic is discussed in the following sections.

4D. Octagonal Structures

A structure consisting of octagons and squares can be obtained by cutting off edges of squares in the standard square structure (Figure 8). The spectrum is asymptotically periodic with a period approximately equal to 15. A very interesting phenomenon is that this structure produces an “almost point” subspectrum. One can detect it either by looking at the dispersion relation and noticing horizontal branches in it, or by noticing high spikes in the graph of the density of states. These spikes look numerically like eigenvalues (sometimes embedded in the continuous spectrum), but we do not believe that’s what they are, though at this moment we cannot prove it. The first such band is located near the value $D = 34$. The others apparently repeat with a period close to 15. This phenomenon is rather unusual for periodic operators. We will discuss its nature in Section 5.

It can be shown using separation of variables that square (or rectangular) geometry does not support this kind of subspectrum. It is interesting therefore

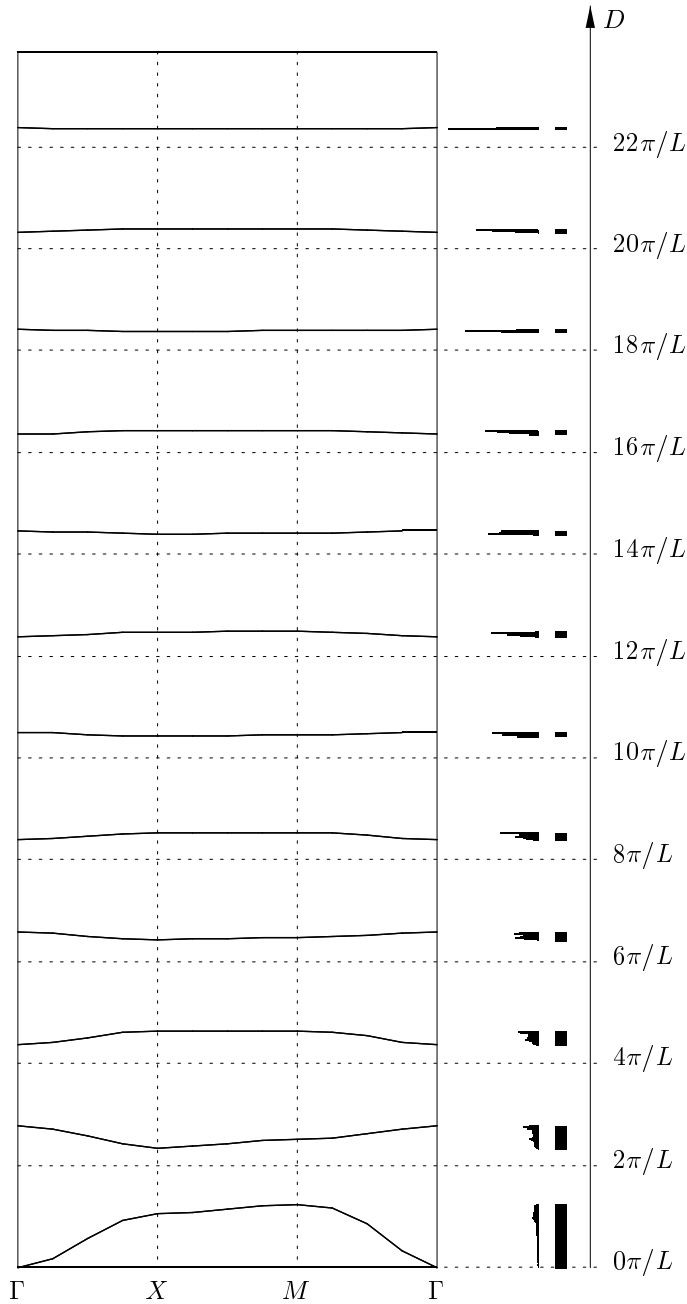
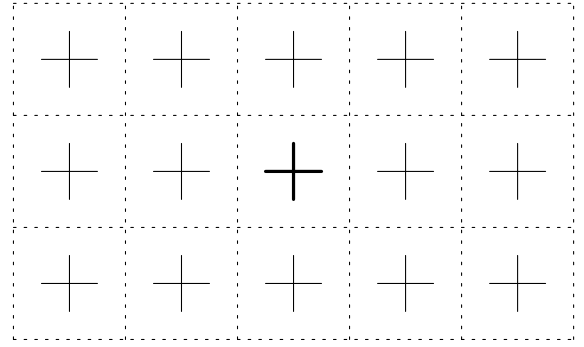
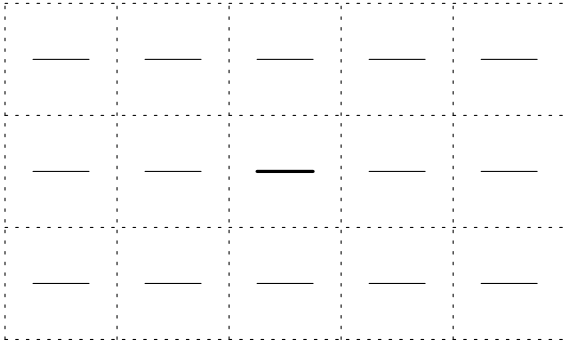


FIGURE 6. A disconnected segment structure and its spectrum. Here $L = 0.5$, the length of the segment.

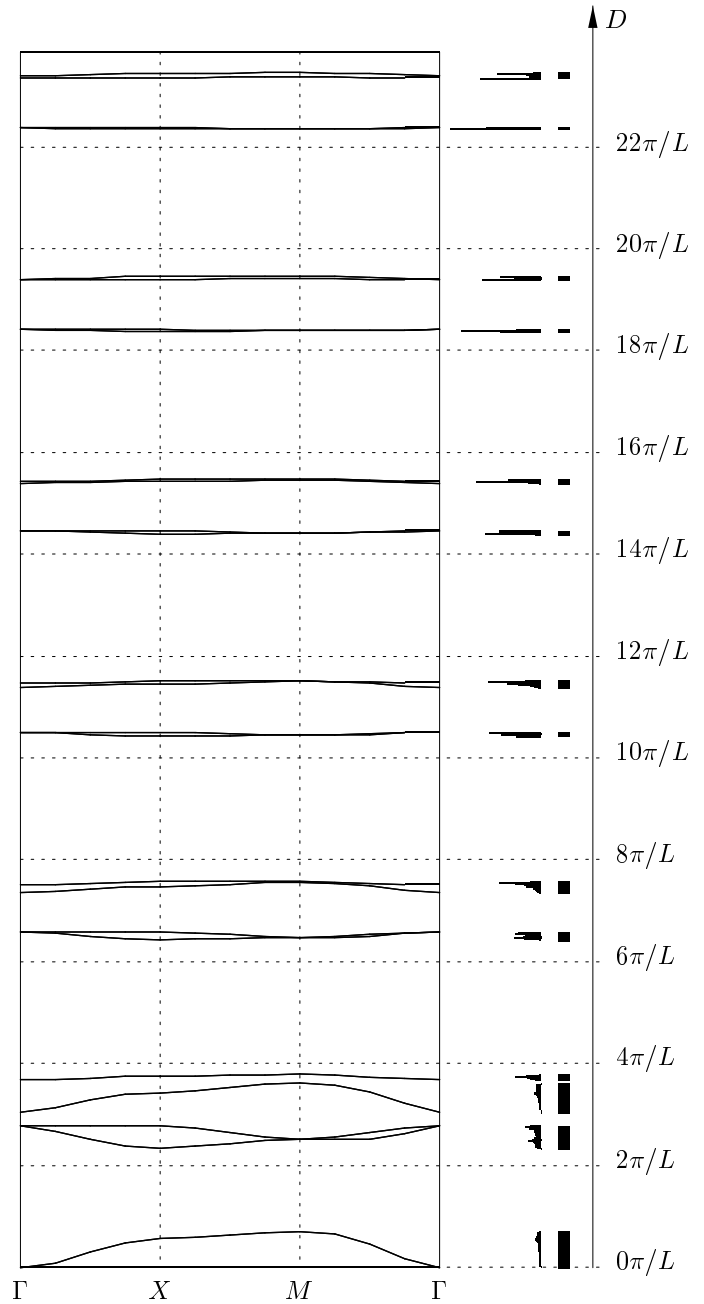


FIGURE 7. A cross structure and its spectrum. Again $L = 0.5$, the diameter of the cross.

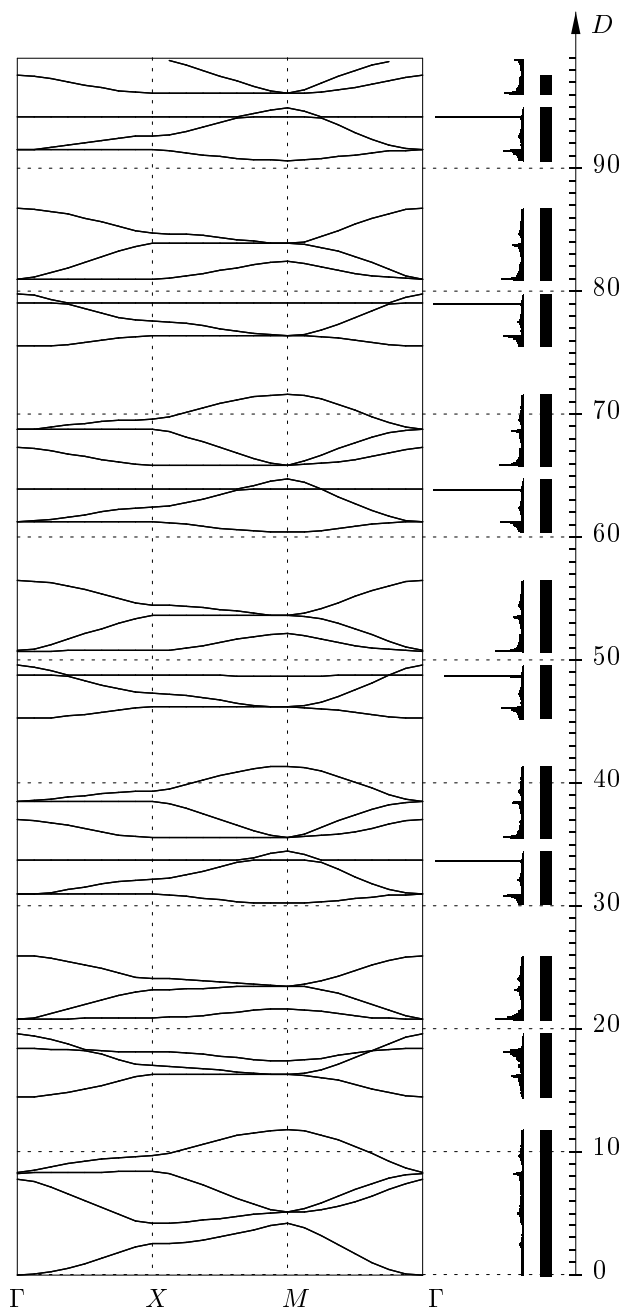
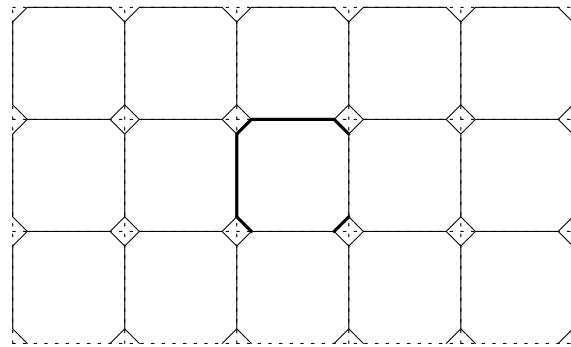
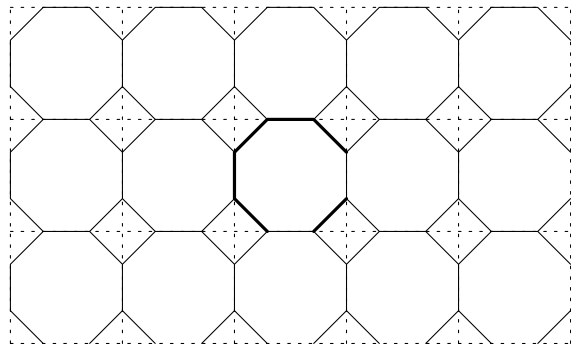


FIGURE 8. A structure made of regular octagons. The spectrum is computed with $\Delta t = 0.00863$.

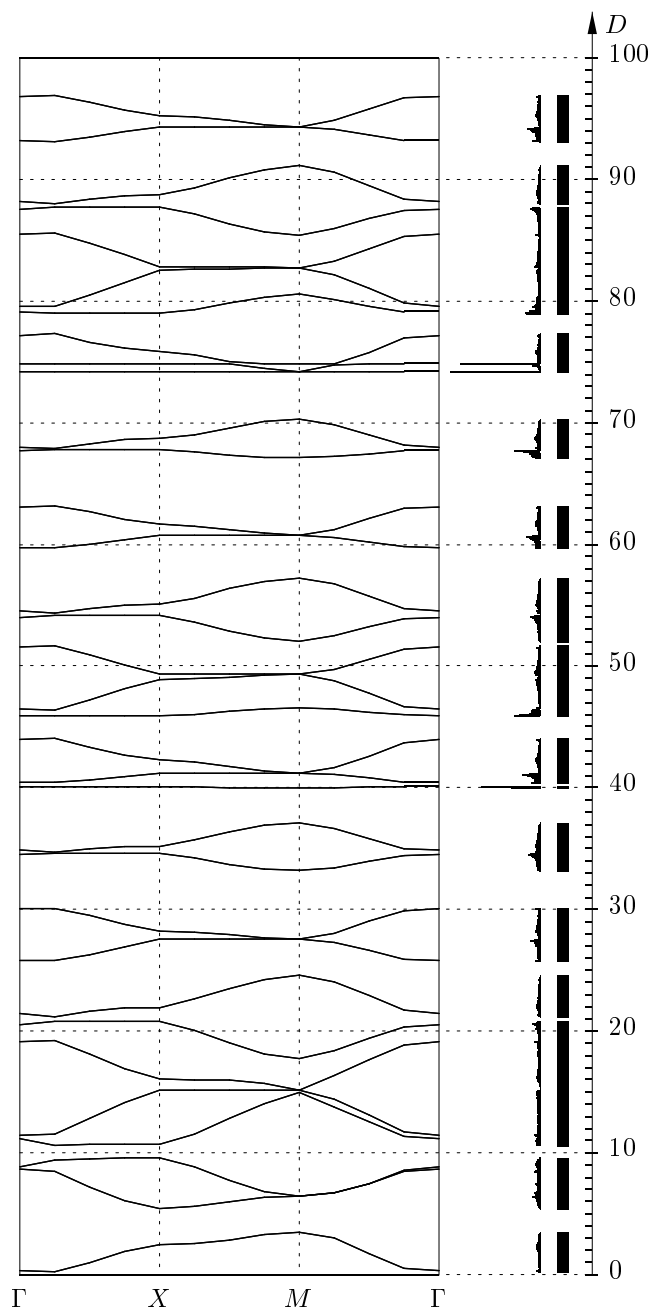


FIGURE 9. A structure made of irregular octagons; long segments are four times the short ones.

to investigate in what way this subspectrum disappears when the size of squares in the octagonal structure becomes very small, so the octagons approach squares. An octagonal structure of this kind is shown in Figure 9, where the long segments are four times the short ones. The spectrum is still asymptotically periodic and has an “almost discrete” component, but the narrow bands are situated much higher in the spectrum. Computations show that when the small squares shrink into points, so the octagons become squares, the narrow bands move higher in the spectrum and apparently disappear at infinity.

4E. Hexagonal Structure

A hexagonal honeycomb structure was generated by six segments of length $s = \sqrt{3}/3$, inscribed into a rectangular cell with a height/width ratio equal to s (Figure 10). Both the “almost point” spectrum and band periodicity can be easily seen. The period is very close to

$$\frac{6\pi}{\sqrt{3}} = \frac{2\pi}{s}$$

and the “almost discrete” bands reside just above the frequencies $2\pi n/s$, for $n = 2, 3, 4, \dots$

Since creating spectral gaps is one of the main goals of photonic crystals research, it is interesting to notice that the hexagonal structure provides smaller density of spectral gaps than the square one.

4F. Connected-Circle Structure

A connected circle structure was generated by sixteen segments as shown in the Figure 11. The circle, of radius 0.25, was approximated by a dodecagon. The narrow bands are repeated with period $4/0.25$. Comparing with the disconnected circle structure, it appears that the “almost point” part of the spectrum in the connected case is a subseries in the spectrum of the disconnected circle structure. We will discuss this phenomenon in Section 5.

4G. Connected-Square Structure

A connected-square structure generated by six segments of equal length, as in Figure 12, shows similar spectral effects. It is asymptotically periodic and contains rather large gaps and a number of narrow “almost point” bands.

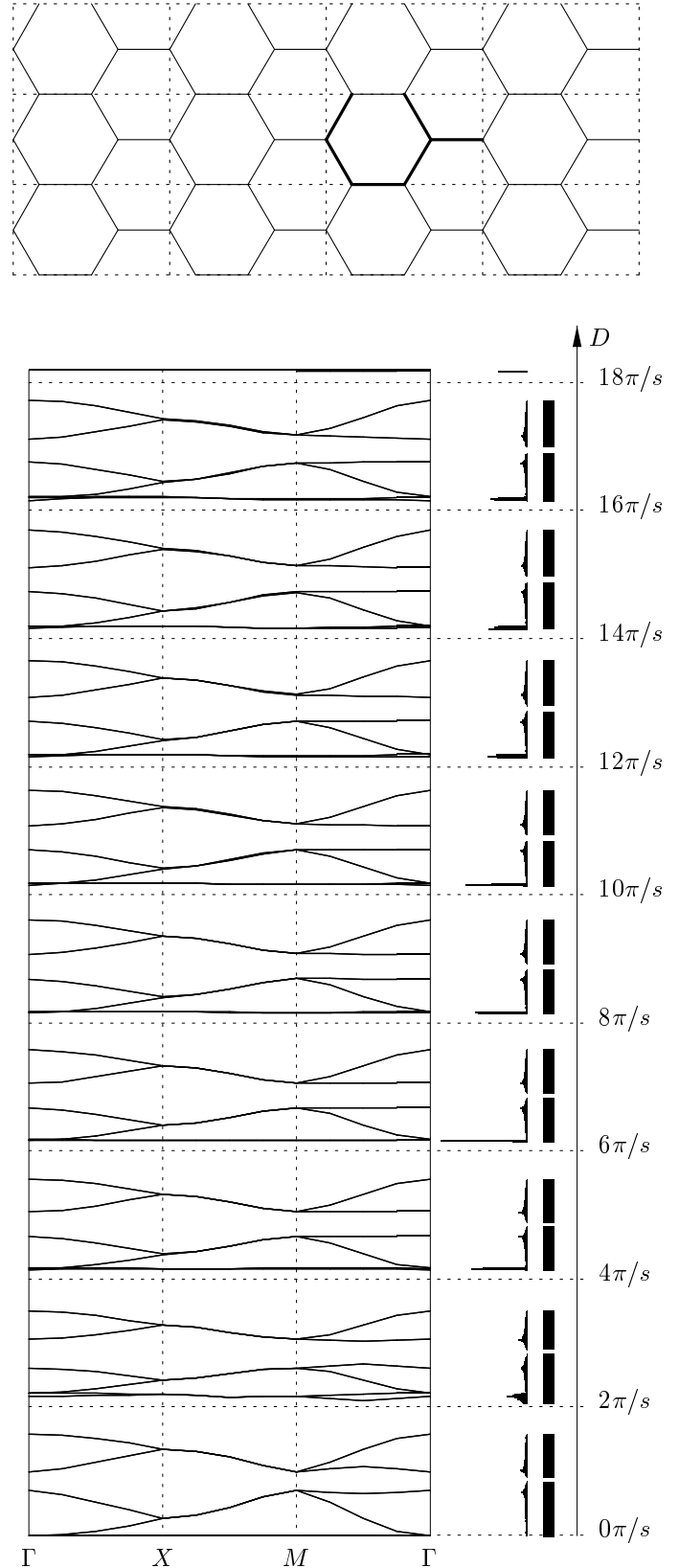


FIGURE 10. A hexagonal structure (honeycomb) and its spectrum. On the vertical axis, $s = 1/\sqrt{3}$ is the height of the unit-width rectangular cells. The spectrum is computed with $\Delta t = 0.0165$ and $\dim \mathbf{A} = 336$.

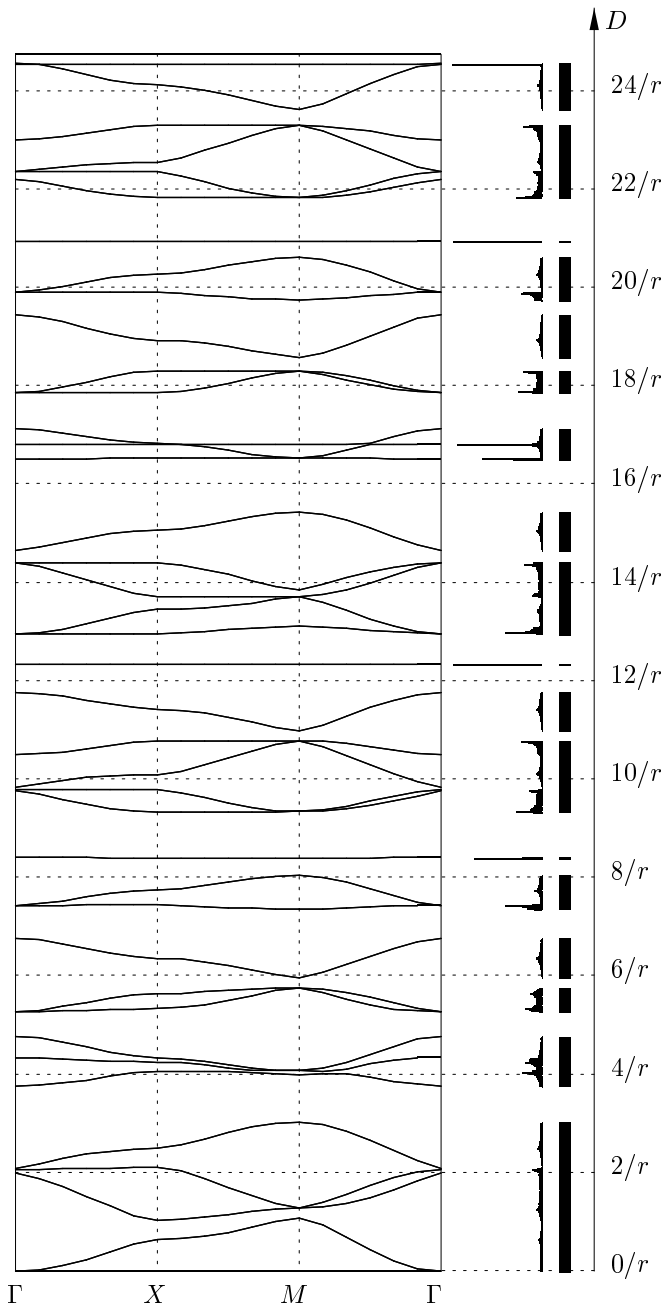
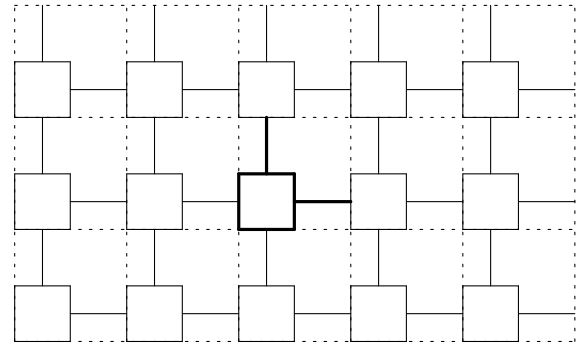
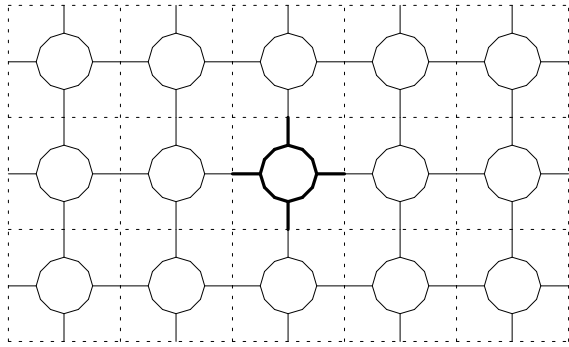


FIGURE 11. Spectrum of structure made of circles of radius $r = 0.25$ connected by segments.

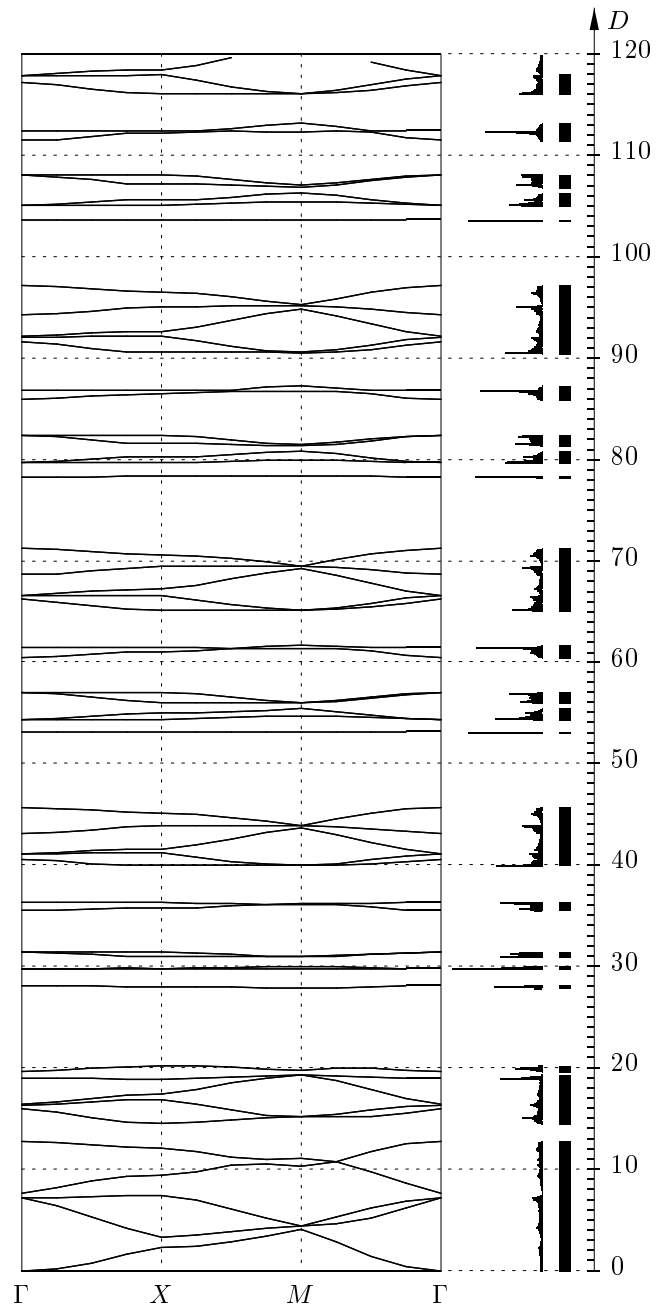


FIGURE 12. Spectrum of structure made of squares of side 0.5 connected by segments.

5. ANALYTIC DISCUSSION OF THE RESULTS

In this section we provide some explanations, sometimes conjectural, for the spectral phenomena described above. Among the interesting properties discovered are the “almost discrete” nature of spectra of disconnected structures, existence of “almost point” (i.e., very narrow) embedded bands, and the periodic nature of spectrum for some geometries.

We start with the square structure, then consider disconnected structures, and conclude the section with the existence of narrow bands for some connected structures.

5A. The Square Structure

As mentioned above, and as discussed in detail in [Figotin and Kuchment 1998b], the square structure can be treated using separation of variables (see analogous considerations in Section 6), and its spectrum can be described by the following transcendental system of inequalities:

$$\left| \cos \eta - \frac{D}{2\eta} \sin \eta \right| \leq 1, \quad \left| \cosh \eta - \frac{D}{2\eta} \sinh \eta \right| \leq 1. \quad (5-1)$$

Here D is the spectral parameter and η is a separation of variables parameter. In other words, D is in the spectrum if and only if there is a value of η such that the pair (D, η) satisfies the system (5-1). This approach was suggested by I. Ponomarev. Figure 13 shows the solutions of the system; the horizontal axis on the picture represents D , and the vertical axis represents the parameter η . The series of “parallel” strips depicts the set of solutions of the first (trigonometric) inequality in (5-1), while a single “diagonal” strip that obviously degenerates into a straight line shows the solution of the second (hyperbolic) inequality. The spectrum corresponds to the D -coordinates of the intersection of the two sets. The vertical lines on the picture correspond to the values $D = n\pi$. It is clear from the picture—and it can be easily proved analytically as in [Figotin and Kuchment 1998b]—that the spectrum very quickly approaches the sequence of intervals of length π separated by gaps of same length. The Dirichlet-to-Neumann operator can be considered as an one-dimensional periodic operator (a pseudodifferential operator on the one-dimensional topological graph Σ). An interesting feature here is that the spectrum becomes asymptotically periodic when $D \rightarrow \infty$. In particular, the

length of gaps does not go to zero, approaching a constant non-zero value instead. This is an unusual property for one-dimensional periodic operators; see [Eastham 1973]. On the other hand, problems of mesoscopic physics lead to some Schrödinger type periodic operators on graphs with singular interactions, whose spectra also show similar effects; see [Avron et al. 1994; Exner 1995].

5B. Disconnected Structures

We believe that the feature of “almost discreteness” of the spectrum of the Dirichlet-to-Neumann operator is common to all disconnected periodic graphs and to more general disconnected surface structures in higher dimensions. We will provide a crude idea of an explanation first, and then elaborate it for the case of smooth disconnected structures.

Let K be a fundamental cell of our periodic structure Σ . If the structure is disconnected, we can choose a cell K in such a way that its boundary has no intersection with the structure. Let the segments S_j belong to the interior of K and constitute the part of the structure Σ that is contained in K . Replicating them by the action of the discrete group Γ of periods, we obtain the whole disconnected structure Σ . Now imagine that we have a non-zero solution $u(x)$ in K of the problem

$$-\Delta u(\mathbf{x}) = D \left(\sum_j \delta_{S_j}(\mathbf{x}) \right) u(\mathbf{x}), \quad (5-2)$$

such that $u = 0$ in a neighborhood of the boundary ∂K of the cell K . In fact, due to standard uniqueness theorems for elliptic equations such a solution cannot exist, but we will ignore this for a moment. If we have such a solution, we can extend it to a Floquet–Bloch solution with any quasimomentum. To do this, we define $u(\mathbf{x})$ as zero outside of the fundamental domain K . Now we can define the function

$$u_{\mathbf{k}}(\mathbf{x}) = \sum u(\mathbf{x} - \gamma) e^{i\mathbf{k} \cdot \gamma}.$$

This function obviously satisfies the equation

$$-\Delta u_{\mathbf{k}}(\mathbf{x}) = D \delta_{\Sigma}(\mathbf{x}) u_{\mathbf{k}}(\mathbf{x})$$

and the Floquet condition with quasimomentum \mathbf{k} . This means that the number D belongs to the spectrum for any quasimomentum. In different terms, there is a constant branch in the dispersion relation. Then standard Floquet theory [Eastham 1973;

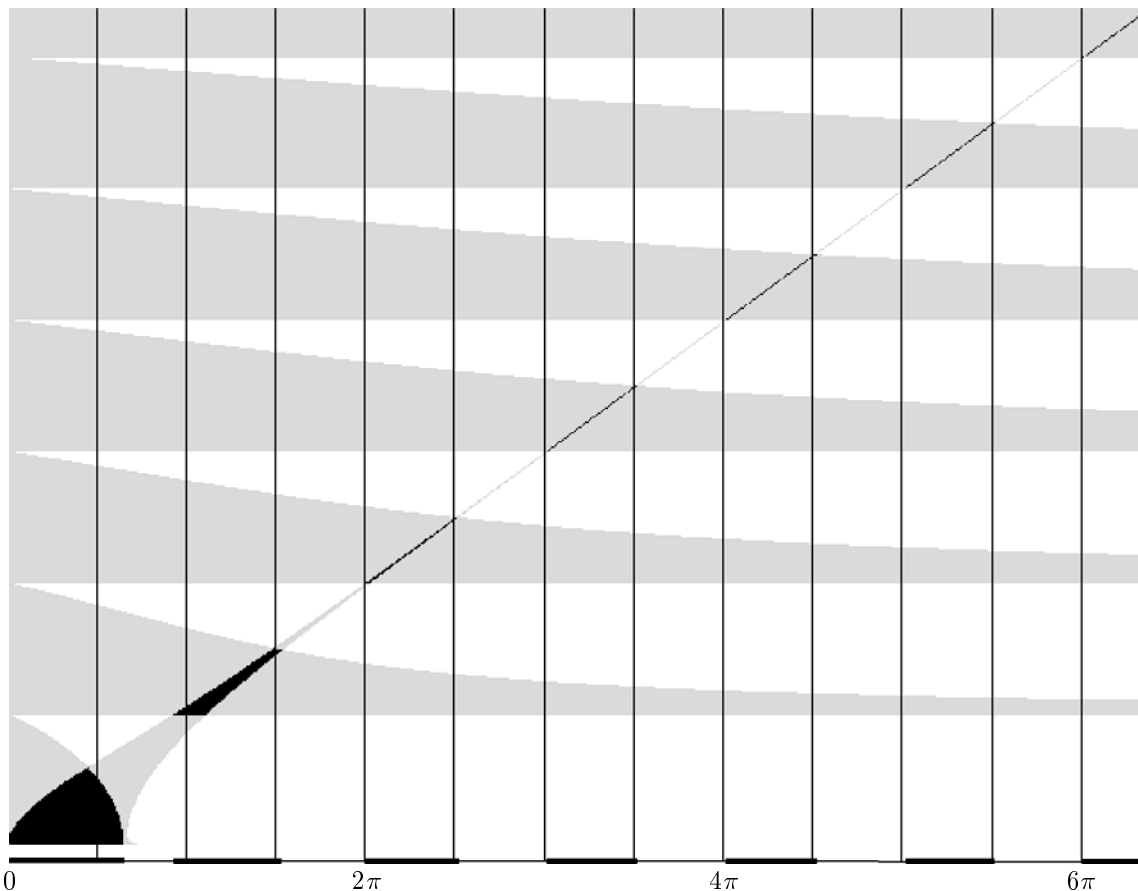


FIGURE 13. Solutions of the transcendental system for the square structure.

Kuchment 1993; Reed and Simon 1978] shows that D belongs to the point spectrum. This explains how existence of a solution with the described properties leads to the point spectrum. The main idea is that the disjoint parts of Σ essentially decouple. However, due to standard elliptic uniqueness theorems such (non-zero) solutions cannot exist. Now recall that, by assumption, the segments S_j do not reach the boundary of K . Results from [Figotin and Kuchment 1995; 1996a; 1996b; 1998a] and some exactly solvable examples suggest that away from the segments S_j the solutions of problem (5-2) decay very fast for large values of D . In other words, if some large value of D belongs to the spectrum, then we have a solution $u(x)$ that is small (though not identically zero) near the boundary of the fundamental domain K . This means that the same solution “almost satisfies” the same problem for arbitrary quasimomentum, and hence the corresponding branch of the dispersion relation is almost constant. This leads to a narrow band of the spectrum and forces the high portions of the spectrum to be almost discrete. This effect becomes more and more

apparent as D increases and different components of Σ decouple.

We make these considerations more precise for the case of a smooth disconnected structure Σ of arbitrary dimension. Let $S \subset \mathbb{R}^m$ be a smooth orientable hypersurface located strictly inside a fundamental domain K of a lattice Γ . Applying translations by elements of Γ to S , one obtains a periodic disconnected structure (surface)

$$\Sigma = \bigcup_{\gamma \in \Gamma} \gamma S \subset \mathbb{R}^m.$$

Let N be the Dirichlet-to-Neumann operator on Σ defined as in Section 2. We are interested in the spectrum of N . Adhering to our previous notations, we denote the spectral variable by D . The next result explains the phenomenon of “almost discreteness” of spectra of disconnected smooth structures like the disconnected circles structure. It also provides asymptotic locations of these spectra and an explanation of their asymptotically periodic nature in 2D. Namely, it states that the spectrum of N at high frequencies concentrates in a small vicinity of

the numbers $2\sqrt{D_n}$, where $\{D_n\}$ is the spectrum of the Laplace–Beltrami operator on S .

Theorem 5.1. *Let $\{D_n\} \subset \mathbb{R}$ be the (discrete) spectrum of the (positive) Laplace–Beltrami operator Δ_S on the closed surface S . There exists a sequence of positive numbers $\rho_n \rightarrow 0$ such that the spectrum of operator N on Σ belongs to the union of intervals*

$$\sigma(N) \subset \bigcup [2\sqrt{D_n} - \rho_n, 2\sqrt{D_n} + \rho_n],$$

and each of these intervals contains a non-empty portion of $\sigma(N)$.

Proof. We sketch the proof over the next three pages, omitting some standard technical details that are easily recoverable.

Denote by T the boundary of the fundamental domain K and by \mathring{K} the interior of K . Consider the Dirichlet boundary value problem

$$\begin{cases} -\Delta u = 0 & \text{in } \mathring{K} \setminus S, \\ u|_S = \varphi, \\ u|_T = 0. \end{cases} \quad (5-3)$$

Now define an operator

$$N_0 : \varphi \rightarrow \left[\frac{\partial \varphi}{\partial \nu} \right]_S, \quad (5-4)$$

where $\left[\frac{\partial \varphi}{\partial \nu} \right]_S$ denotes the jump of the normal derivative of function φ across S , that is, the sum of outer normal derivatives from both sides of S . Standard results on the Calderón projector (see [Sylvester and Uhlmann 1988, Theorem 0.1], for instance) imply the following statement.

Lemma 5.2. *The operator N_0 is a classical pseudodifferential operator of order 1. Moreover, its symbol shows that*

$$N_0 = 2\sqrt{\Delta_S} + R,$$

where R is a smoothing operator.

Perturbation arguments show that asymptotically (for large eigenvalues) the spectrum of N_0 behaves as $\{2\sqrt{D_n}\}$. Now we only have to deduce that the spectrum of N concentrates around the spectrum of N_0 . To do this we need the following auxiliary statement, which formalizes our heuristic considerations made in the beginning of this section.

Lemma 5.3. *Let $u_D \in L_2(S)$ be a normalized eigenfunction of the operator N_0 , with eigenvalue D . Extend u_D to all of K as a solution of (5-3), using*

u_D as the Dirichlet boundary value φ . Let U be a neighborhood of T in K such that $S \cap \bar{U} = \emptyset$. Then

$$|u_D(x)| \leq CD^{-1}, \quad \text{for } x \in U. \quad (5-5)$$

Proof. First of all, since $u_D = 0$ on T , the maximum principle implies that it is sufficient to prove estimate (5-5) away from T . In other words, it is possible to assume that $(S \cup T) \cap \bar{U} = \emptyset$. A solution $u(x)$ of problem (5-3) can be described in $\mathring{K} \setminus S$ by means of a kernel (Green’s function of the Dirichlet boundary value problem):

$$u(x) = \int_S F(x, y) \varphi(y) dy,$$

where $F(x, y)$ as a function of $(x, y) \in U \times S$ is smooth (we need to recall here that $(S \cup T) \cap \bar{U} = \emptyset$). In particular,

$$\|F(x, \cdot)\|_{H^1(S)} \leq \text{const}, \quad \text{for } x \in U. \quad (5-6)$$

Now consider the solution u_D in U :

$$\begin{aligned} u_D(x) &= \int_S F(x, y) u_D(y) dy \\ &= \frac{1}{D} \int_S F(x, y) N_0^y u_D(y) dy \\ &= \frac{1}{D} \int_S N_0^y F(x, y) u_D(y) dy, \end{aligned}$$

where the operator N_0^y stands for N_0 acting with respect to variable y . Here we have used the self-adjointness of this operator, the equality $N_0 u_D = D u_D$, and the inclusion $F(x, \cdot) \in \mathcal{D}(N_0) = H^1(S)$ for $x \in U$. This representation, the normalization of u_D , the estimate (5-6), the fact that N_0 is a pseudo-differential operator of order one, and the Cauchy–Schwartz inequality imply (5-5):

$$\begin{aligned} |u_D(x)| &\leq D^{-1} \|N_0^y F(x, y)\|_{L_2(S)} \|u_D\|_{L_2(S)} \\ &\leq CD^{-1} \max\{\|F(x, \cdot)\|_{H^1(S)} : x \in U\} \\ &\leq C_1 D^{-1}. \quad \square \end{aligned}$$

The next statement follows from this lemma and standard interior elliptic estimates.

Lemma 5.4. *In any subdomain $V \subset K$ such that \bar{V} is disjoint from $T \cup S$ we have*

$$\|u_D\|_{H^r(V)} \leq C_r D^{-1} \quad (5-7)$$

for the Sobolev space $H^r(V)$ of any order r .

Now choose a quasi-momentum \mathbf{k} . Then, imposing Floquet conditions on T with this quasimomentum instead of zero Dirichlet conditions, one defines an

operator $N(\mathbf{k})$, which is also a pseudodifferential operator on S :

$$N(\mathbf{k})\varphi = \left[\frac{\partial u}{\partial n} \right] \Big|_S,$$

where u is the solution of the problem

$$\begin{cases} -\Delta u = 0 & \text{in } \dot{K} \setminus S, \\ u|_S = \varphi & \text{on } S, \\ u(x + \gamma) = e^{i\gamma \cdot \mathbf{k}} u(x) & \text{on } T, \\ \left. \frac{\partial u(x + \gamma)}{\partial n} \right|_T = e^{i\gamma \cdot \mathbf{k}} \left. \frac{\partial u(x)}{\partial n} \right|_T & \text{on } T. \end{cases} \quad (5-8)$$

Floquet theory [Kuchment 1993; Reed and Simon 1978] claims that

$$\sigma(N) = \cup_{\mathbf{k} \in B} \sigma(N(\mathbf{k})),$$

where B is the Brillouin zone introduced before.

We now need to establish some simple properties of problem (5-8).

Lemma 5.5. *For any \mathbf{k} in the Brillouin zone the homogeneous problem (5-8) (i.e., with $\varphi = 0$) has only the trivial solution $u = 0$.*

Proof. Consider the spectral problems $M(\mathbf{k})$ given by

$$\begin{cases} -\Delta u = \lambda u & \text{in } \dot{K} \setminus S, \\ u|_S = 0 & \text{on } S, \\ u(x + \gamma) = e^{i\gamma \cdot \mathbf{k}} u(x) & \text{on } T, \\ \left. \frac{\partial u(x + \gamma)}{\partial n} \right|_T = e^{i\gamma \cdot \mathbf{k}} \left. \frac{\partial u(x)}{\partial n} \right|_T & \text{on } T. \end{cases} \quad (5-9)$$

The claim of the lemma is that the spectrum of the problem $M(\mathbf{k})$ does not contain zero for any $\mathbf{k} \in B$. Now introduce the Dirichlet Laplacian $(-\Delta_{\Sigma,D})$ in $\mathbb{R}^n \setminus \Sigma$ with Dirichlet conditions on the periodic surface Σ (we recall that Σ consists of disjoint replicas of S). As follows from Floquet theory [Kuchment 1993; Reed and Simon 1978], the spectrum of this operator can be described as

$$\sigma(-\Delta_{\Sigma,D}) = \bigcup_{\mathbf{k} \in B} \sigma(M(\mathbf{k})).$$

Hence, our goal is to show that $\sigma(-\Delta_{\Sigma,D})$ does not contain zero. Denote by Ω the unique unbounded (and periodic) connected component of the open set $\mathbb{R}^n \setminus \Sigma$ and by Ω_1 its complement in $\mathbb{R}^n \setminus \Sigma$. Then the operator $-\Delta_{\Sigma,D}$ splits into the direct sum of two Dirichlet Laplacians, in Ω and Ω_1 respectively. The domain Ω_1 is the union of a periodic array of bounded domains, so the maximum principle implies that the Dirichlet Laplacian $-\Delta_{\Omega_1,D}$ has a strictly

positive spectrum. What remains to show is that $0 \notin \sigma(-\Delta_{\Omega,D})$. To do so, we first notice that operator $(-\Delta_{\Omega,D})$ has only essential spectrum; this can easily be shown by taking into account periodicity and selfadjointness (using arguments similar to the ones in the proof of [Eastham 1973, Theorem 6.10.1]). In the terminology of [Glazman 1966] and [Edmunds and Evans 1987], Ω is a quasi-cylindrical domain. In particular, Theorem 6.7 of Chapter X of this last reference applies, and implies that the essential spectrum of $(-\Delta_{\Omega,D})$ is bounded from below by a positive constant. \square

We are now able to prove an analog of Lemmas 5.3 and 5.4 for operators $N(\mathbf{k})$.

Lemma 5.6. *Let $u_D \in L_2(S)$ be a normalized eigenfunction of the operator $N(\mathbf{k})$ (where $\mathbf{k} \in B$) with eigenvalue D . Extend u_D to the whole K as a solution of (5-8), using u_D as the Dirichlet boundary value φ . Let U be an open subdomain of K such that $(S \cup T) \cap \bar{U} = \emptyset$. Then*

$$\|u_D\|_{H^r(U)} \leq CD^{-1}, \quad (5-10)$$

where the constant C does not depend on $\mathbf{k} \in B$.

Proof. Lemma 5.5 implies existence of Green's functions $F(x, y, \mathbf{k})$ smoothly depending on $\mathbf{k} \in B$. Now the proofs of Lemmas 5.3 and 5.4 can be repeated with all estimates uniform with respect to \mathbf{k} . \square

We will show now that for large eigenvalues and for any quasimomentum \mathbf{k} the spectrum of $N(\mathbf{k})$ is located close to the spectrum of N_0 . This implies closeness of $\sigma(N)$ and $\sigma(N_0)$.

Lemma 5.7. *If $D \in \sigma(N_0)$ and u_D is the corresponding eigenfunction, the following estimate holds uniformly with respect to \mathbf{k} :*

$$\|(N(\mathbf{k}) - D)u_D\|_{L_2(S)} \leq CD^{-1}.$$

Proof. To define $N(\mathbf{k})u_D$, we have to solve problem (5-8) with $\varphi = u_D$. Let $U \subset K$ be an open "shell" domain such that $(S \cup T) \cap \bar{U} = \emptyset$ and such that S and T belong to different connected components of $K \setminus \bar{U}$. Consider a smooth cut-off function ψ that is equal to 1 in a neighborhood of S , is equal to zero in a neighborhood of T , and differs from 1 and 0 inside U . Set $q(x) = u_D(x)\psi(x)$. Then this function satisfies both boundary conditions in (5-8), but does not satisfy the Laplace equation. However,

our estimate (5–7) implies that the function $p(x) = -\Delta q(x)$ satisfies, for any r , the estimate

$$\|p\|_{H^r(K)} \leq C_r D^{-1}.$$

Now consider the problem

$$\begin{cases} -\Delta u = -p & \text{in } \overset{\circ}{K} \setminus S, \\ u|_S = 0 & \text{on } S, \\ u(x + \gamma) = e^{i\gamma \cdot \mathbf{k}} u(x) & \text{on } T, \\ \left. \frac{\partial u(x + \gamma)}{\partial n} \right|_T = e^{i\gamma \cdot \mathbf{k}} \left. \frac{\partial u(x)}{\partial n} \right|_T & \text{on } T. \end{cases} \quad (5-11)$$

According to Lemma 5.5, this problem has a unique solution. Let V be an open neighborhood of S such that $\bar{V} \cap T = \emptyset$. Then the function u can be estimated uniformly with respect to \mathbf{k} according to standard estimates for elliptic boundary value problems as

$$\|u\|_{H^2(V \setminus S)} \leq CD^{-1}.$$

In particular,

$$\left\| \left[\frac{\partial u}{\partial \nu} \right] \right\|_{L_2(S)} \leq CD^{-1}.$$

Now

$$(N(\mathbf{k}) - D)u_D = \left[\frac{\partial u_D}{\partial \nu} \right] - Du_D + \left[\frac{\partial u}{\partial \nu} \right] = \left[\frac{\partial u}{\partial \nu} \right],$$

which finishes the proof of the lemma. \square

Since $N(\mathbf{k})$ is self-adjoint, the norm of its resolvent can be estimated from above by the inverse distance to the spectrum of $N(\mathbf{k})$. Hence, the lemma implies existence of a sequence $\rho_n \rightarrow 0$ such that intervals of half-length ρ_n centered at D_n contain elements from the spectra of $N(\mathbf{k})$ for all \mathbf{k} .

Corollary 5.8. *In a ρ_n -vicinity of an eigenvalue D_n of N_0 there are points from the spectra of all operators $N(\mathbf{k})$. Here $\rho_n \rightarrow 0$ when $n \rightarrow \infty$.*

Now our arguments can be reversed: starting with $N(\mathbf{k})$ one can show the existence of a sequence $\rho'_n \rightarrow 0$ independent of $\mathbf{k} \in B$ such that intervals of half-length ρ'_n centered at eigenvalues of $N(\mathbf{k})$ contain elements from the spectrum of N_0 .

Corollary 5.9. *For any $\mathbf{k} \in B$ there are points from the spectrum of N_0 in a ρ'_n -vicinity of an eigenvalue $D_n(\mathbf{k})$ of $N(\mathbf{k})$. Here $\rho'_n \rightarrow 0$ when $n \rightarrow \infty$.*

These two corollaries imply that the spectrum of the operator N is asymptotically close to that of the operator N_0 . Since, as explained before, the spectrum of N_0 is asymptotically close to $\{2\sqrt{D_n}\}$, this finishes the proof of the theorem. \square

Remark 5.10. In fact, if S is smooth, one can guarantee that

$$\rho_n \leq c_p D_n^{-p}$$

for any p . This can be easily achieved by repeating the arguments of Lemma 5.3. The case when S is a circle can be solved explicitly using Fourier series. It shows that analyticity of S probably implies exponential decay of ρ_n .

Theorem 5.1 explains the ‘‘almost discreteness’’ and location of the spectrum for disconnected smooth structures. For instance, in the 2D case we conclude that the spectrum at higher frequencies must concentrate around the values $4\pi nL^{-1}$, where L is the length of S . In particular, for a circle of radius R this leads to $2n/R$, which agrees perfectly with our numerical results described before. This also provides an explanation of the asymptotic periodicity of the spectrum that was observed in numerics. Numerics also suggests that although the theorem has an asymptotic nature (i.e., it works for high eigenvalues), the asymptotic convergence is very fast and works even for rather low eigenvalues.

Another important feature of this theorem is that it describes asymptotically the spectrum of a pseudo-differential problem in terms of a differential one, which is much simpler to study.

It is interesting and important to study similar effects for non-smooth disconnected structures (the ones that have corners, loose ends, and graph vertices). We conjecture in particular that an analog of Theorem 5.1 could explain the asymptotic behavior of spectra for some non-smooth disconnected structures. However, the numerics suggests that non-smooth structures present some new features that still need to be understood. For instance, making S non-smooth changes the spectrum of S significantly, although our initial guess was that only the rate of convergence to numbers $4\pi n/L$ would be smaller. Computing the spectrum for the case of disjoint squares (Figure 14), one discovers that apparently the formula $4\pi n/L$ (where L is the perimeter of the square) no longer predicts the approximate locations of the spectral bands. Moreover, considering rectangles with the same perimeter but with different aspect ratios, one discovers that the spectra differ significantly. The example of a single-segment disconnected periodic structure (Figure 6) shows that although the formula $4n\pi/L$ does give an approximate idea about the location of bands (if one thinks

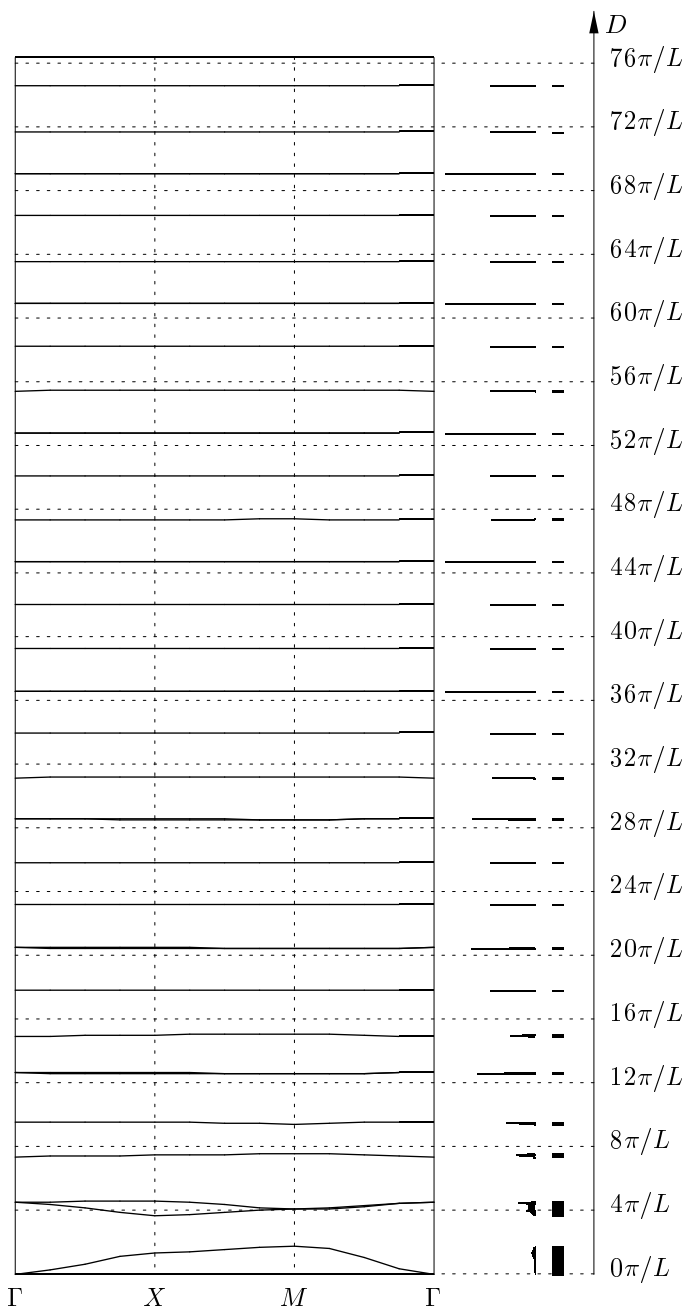
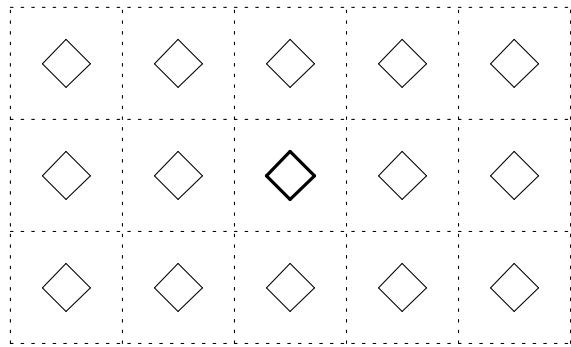


FIGURE 14. Spectrum of structure made of squares with perimeter $L = 1.2$.

of the segment as two-sided, therefore doubling its length), there is some regular discrepancy associated with this formula. The question is, what (if any) “Laplace–Beltrami” operator on a segment (or on a more general graph) describes correctly the asymptotics of our photonic spectrum? Some preliminary considerations suggest that the boundary conditions at the ends of the segment must also contain the spectral parameters in order to agree with the numerical results. It is not quite clear yet how one can treat more complex structures involving vertices or corners. It is also not known whether a differential problem on a general periodic graph can provide the asymptotics for the photonic spectrum. If the answer were yes, this probably would lead to closer ties with the study of problems of mesoscopic physics, where such differential operators customarily arise (see [Exner and Seba 1989] and references therein). So, analytic consideration of the case of non-smooth disconnected structures is still an unsolved problem. We plan to treat it elsewhere.

5C. Connected Structures: “Almost Point” Spectra and Localization

If one wants to understand the phenomenon of the “almost point” spectrum that sometimes arises in connected structures (see discussion in Section 4 above), the natural idea is to look at the corresponding eigenmodes. Since L_2 -eigenvalues (i.e., the point spectrum) correspond to the localized states, also known as bounded states, one can expect that the effect of “almost point” spectrum could also be related to some localization of waves. Figure 15 shows in grey scale the absolute values of the first and second eigenmodes that correspond to the narrow bands of the spectrum of the connected circle structure. Figure 16 contain similar pictures for the connected-square and hexagonal structures. In all cases it is obvious that the waves are rather strongly localized. In the case of the connected circle structure the wave runs around the circle, in the square case it runs around the square, and in the hexagonal case it seems to be reflecting from the endpoints of an edge of the structure and hence staying mostly inside this edge. It is not hard to show that at the locations of these narrow bands one can create an “almost eigenfunction” supported in the fundamental domain of the periodic structure. (By this we mean a normalized function φ such that $\|(N - D)\varphi\| < \varepsilon_D \|\varphi\|$,

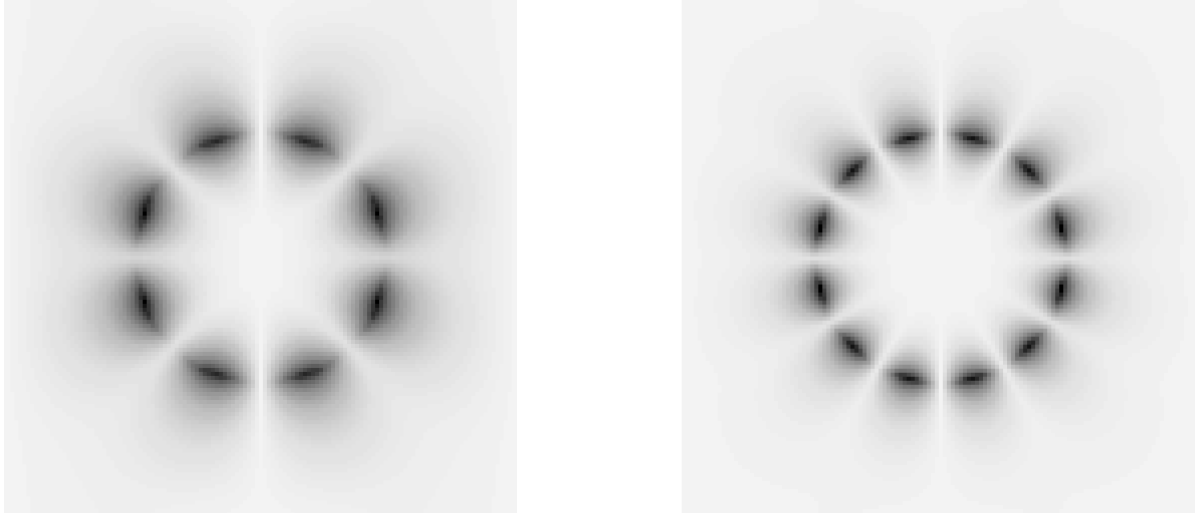


FIGURE 15. The first and second localized eigenmodes of the connected circle structure.

where D is located in a narrow zone and $\varepsilon_D \rightarrow 0$ when $D \rightarrow \infty$.)

The waves corresponding to the wide bands do not show such localized patterns. This raises the following natural model: We keep only the part of the graph where the wave is localized and translations of this part along the group of periods. This creates a disconnected structure. Consider its spectrum. The natural guess is that the “almost point” spectrum of the connected structure must resemble a part (or the whole) of the spectrum of the corresponding disconnected structure. We show below that this model is supported by our numerical results. In some cases we are able to explain the phenomenon of narrow bands and predict their location by means of some symmetry arguments.

Consider the connected-circle structure Σ shown in Figure 11 and denote by N the corresponding Dirichlet-to-Neumann operator, whose spectrum we are interested in. Choose the coordinate system centered at the center of one of the circles, which we call S , and direct the coordinate axes along the connecting edges of the structure. Then the structure becomes symmetric with respect to both axes, with group of symmetry $G = \mathbb{Z}_2 \times \mathbb{Z}_2$ generated by mirror reflections about the axes. Eliminating the connecting edges, we obtain a disconnected structure Σ_1 consisting of circles, which has the same symmetry group. The corresponding Dirichlet-to-Neumann operator will be denoted by N_1 . As was established in Theorem 5.1, the spectrum $(2\pi n/L)^2$ of the (positive) Laplace–Beltrami operator Δ_S on

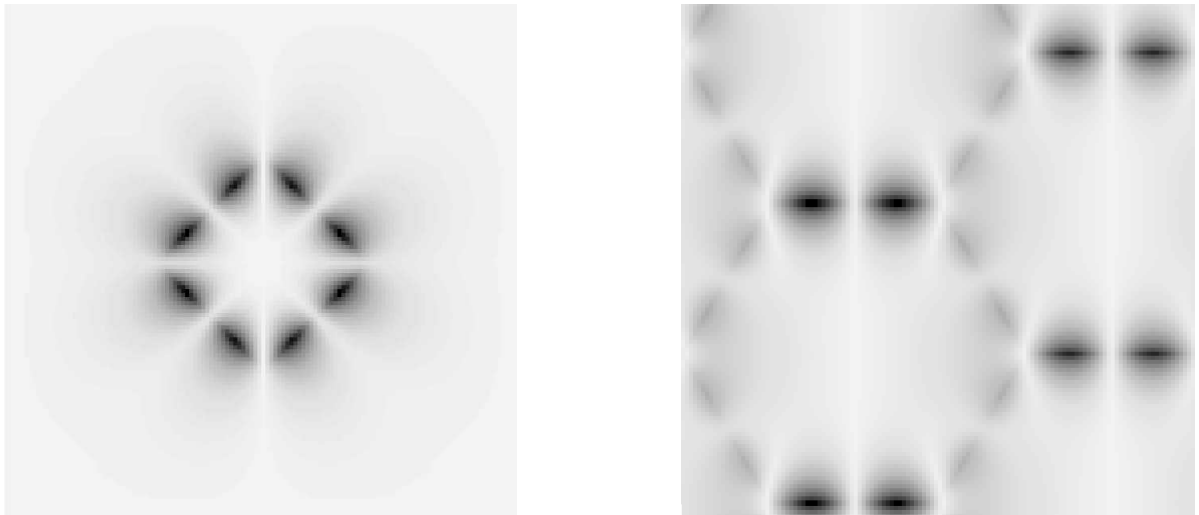


FIGURE 16. The first localized eigenmode of the octagonal (left) and honeycomb (right) structures.

the circle S leads to the spectral bands of the operator N_1 that are located close to numbers $4\pi n/L$. The eigenfunctions of Δ_S can be classified according to the irreducible representations of the group G ; those of N_1 can be classified in a similar way. Let D_n be a series of eigenvalues of Δ_S that correspond to eigenfunctions that adhere to some fixed irreducible representation of G . The arguments in the proof of Theorem 5.1 were G -invariant. As the result, the bands of the spectrum of N_1 that concentrate around the numbers $2\sqrt{D_n}$ contain some Floquet eigenmodes with the same symmetry. In fact, the proof of the theorem also shows that both the operator N_0 of (5-4) and a similar operator with Neumann conditions on T have eigenvalues close to $2\sqrt{D_n}$ and such that the corresponding eigenfunctions have the same symmetry. Consider the eigenfunctions that are antisymmetric with respect to both coordinate axis. It is easy to see that they correspond to the eigenvalues $(4\pi n/L)^2$ of Δ_S . The corresponding bands of the spectrum of operator N_1 are located around the numbers $8\pi n/L$. We will show now that δ -type spikes must appear close to these numbers in the density of states of the Dirichlet-to-Neumann operator N for the connected structure Σ . In fact, we will deal with the (yet to be defined) integrated density of states $\mathcal{N}(\lambda)$ of the operator N . This claim is based on a simple observation:

Lemma 5.11. *If an eigenfunction of the operator N_1 for the disconnected structure is antisymmetric with respect to both axes, then it is also an eigenfunction (with the same eigenvalue) of the operator N (for the connected structure).*

Proof. Denote by Σ_c the union of the circles of our structure, and by Σ_e the union of all connecting edges. Then an eigenfunction u of N that corresponds to an eigenvalue D must satisfy the conditions

$$\begin{cases} -\Delta u = 0 & \text{in } \mathbb{R}^2 \setminus (\Sigma_c \cup \Sigma_e), \\ [\partial u / \partial \nu] = Du & \text{on } \Sigma_c, \\ [\partial u / \partial \nu] = Du & \text{on } \Sigma_e, \end{cases} \quad (5-12)$$

where $[\partial u / \partial \nu]$ denotes the jump of the normal derivative. On the other hand, an eigenfunction of N_1 satisfies

$$\begin{cases} -\Delta u = 0 & \text{in } \mathbb{R}^2 \setminus \Sigma_1, \\ [\partial u / \partial \nu] = Du & \text{on } \Sigma_c, \\ [\partial u / \partial \nu] = 0 & \text{on } \Sigma_e. \end{cases} \quad (5-13)$$

Here the condition on Σ_e follows from the harmonicity (and hence smoothness) of u across Σ_e . Now, an antisymmetric solution of (5-13) is automatically equal to zero on Σ_e , and hence it also satisfies (5-12). \square

We will assume as before (without loss of generality) that the group of periods is the integer lattice \mathbb{Z}^2 . Denote by V_n a sequence of concentric squares with sides of size v_n parallel to the coordinate axes, with $v_n \rightarrow \infty$. Assume also that the boundary of V_n does not contain any vertices of the graph Σ and intersects Σ transversely at its edges. One can now define a bounded from below self-adjoint Dirichlet-to-Neumann operator N_{V_n} on $\Sigma_n = \Sigma \cap V_n$ as follows:

$$N_{V_n} \varphi = \left[\frac{\partial u}{\partial \nu} \right] \Big|_{\Sigma_n},$$

where u is a periodic function in \mathbb{R}^2 with fundamental cell V_n and satisfying the problem

$$\begin{cases} -\Delta u = 0 & \text{in } V_n \setminus \Sigma_n, \\ u = \varphi & \text{on } \Sigma_n. \end{cases} \quad (5-14)$$

It is not hard to justify that this operator has a discrete spectrum. This enables one to define for this operator an integrated density of states function as the eigenvalue counting function: $\mathcal{N}_{V_n}(\lambda)$ is the number of eigenvalues $D \leq \lambda$ of N_{V_n} , where eigenvalues are counted with their multiplicity. It should be possible to generalize Theorem 2.1 of [Shubin 1979], which claims the existence of a weak limit when $n \rightarrow \infty$ of the functions $\mathcal{N}_{V_n}(\lambda)$ normalized to the volume of V_n :

$$\mathcal{N}(\lambda) = \lim v_n^{-2} \mathcal{N}_{V_n}(\lambda).$$

This limit should naturally be called the integrated density of states of operator N . The appropriate notion of a weak limit can be found in [Shubin 1979, Section 2.1]. For the task we are pursuing now it is not worth going into the details of such a theory. Instead, we formulate a result in terms of the distribution functions $\mathcal{N}_{V_n}(\lambda)$. This result explains the δ -type spikes close to points $4n/r$ in the density of states $d\mathcal{N}(\lambda)/d\lambda$ (if such a derivative exists).

Theorem 5.12. *There are numbers $\rho_n \rightarrow 0$ such that*

$$\liminf \left(\mathcal{N}_{V_m} \left(\frac{4n}{r} + \rho_n \right) - \mathcal{N}_{V_m} \left(\frac{4n}{r} - \rho_n \right) \right) \geq 1, \quad (5-15)$$

where the limit is considered for $m \rightarrow \infty$ and r is the radius of the circle S defining the connected circle structure.

Proof. Consider the sequence $\{\psi_n\}$ of antisymmetric eigenfunctions of Δ_S corresponding to the eigenvalues $(2n/r)^2$. Then the solution of the Dirichlet problem

$$\begin{cases} -\Delta u_n = 0 & \text{in } K \setminus (S \cup T), \\ u_n = \psi_n & \text{on } S, \\ u_n = 0 & \text{on } T, \end{cases} \quad (5-16)$$

is also antisymmetric. An estimate similar to the one in Lemma 5.4 shows that this solution decays on any open subset disjoint with S and T as n tends to ∞ . Then the Dirichlet-to-Neumann operator N_0 of (5-4) satisfies

$$(N_0 - 4n/r)\psi_n = 2(\sqrt{\Delta_S} - (2n/r))\psi_n + R\psi_n,$$

with a smoothing operator R . We can conclude that

$$\|(N_0 - 4n/r)\psi_n\|_{L_2(S)} \rightarrow 0.$$

As explained in Lemma 5.11, the same function ψ_n , extended by zero over the edges of the connected structure, provides an approximate eigenfunction for the Dirichlet-to-Neumann operator N_0 on the connected structure too (since ψ_n is equal to zero along the edges). Due to the decay of u_n away from S , considerations analogous to the ones in Lemma 5.7 and Corollary 5.8 show that

$$\|(N(\mathbf{k}) - 4n/r)\psi_n\|_{L_2(S)} \rightarrow 0$$

uniformly with respect to $\mathbf{k} \in B$. This shows the existence of a sequence $\rho_n \rightarrow 0$ such that any segment $(4n/r - \delta_n, 4n/r + \delta_n)$ contains eigenvalues of $N(\mathbf{k})$ (for the connected structure) for arbitrary $\mathbf{k} \in B$. Now consider the operator N_{V_m} . Any eigenfunction of $N(\mathbf{k})$ with $\mathbf{k} = (2\pi l/v_m, 2\pi t/v_m)$, for integer l and t , is an eigenfunction of N_{V_m} . Since the segment $(4n/r - \delta_n, 4n/r + \delta_n)$ contains eigenvalues of $N(\mathbf{k})$ for arbitrary $\mathbf{k} \in B$, in particular for any $\mathbf{k} = (2\pi l/v_m, 2\pi t/v_m) \in B$, we get for $m \rightarrow \infty$ the inequality

$$\liminf (N_{V_m}(4n/r + \rho_n) - N_{V_m}(4n/r - \rho_n)) \geq 1,$$

which proves the theorem. \square

The theorem explains the existence and predicts well the asymptotic location of all numerically discovered high spikes in the density of states for the connected-circle structure. Similar symmetry considerations can be provided for some other structures, like the octagonal or connected-squares ones: eigenvalues corresponding to the antisymmetric eigenfunctions of the disconnected structure indicate the location

of spikes of the density state for the connected one. Numerics confirms this analytic result.

Our whole approach was based on symmetry. It is not clear, however, how important the symmetry is. Can the effect survive when the symmetry is destroyed? It would also be nice to have an explanation of this effect for the honeycomb structure and of its non-existence for the square structure. Numerics shows that the δ -type spikes in the density of states for the honeycomb structure occur close to the location of some narrow spectral bands of the disconnected one-segment structure obtained by eliminating all non-horizontal edges of the honeycomb structure. This shows that some part of the above considerations should survive for this geometry too.

6. COMPARING 2D AND HIGHER DIMENSIONAL CASES

As shown in [Figotin and Kuchment 1996a; 1995; 1998a; 1996b] (and also as a consequence of the study presented in this paper), there are many possibilities for opening spectral gaps in 2D photonic crystals. In particular, many geometries provide an infinite number of gaps in the spectrum of the Dirichlet-to-Neumann operator studied above. We will see now that the situation is completely different in dimensions three and higher. We believe that the following statement holds:

Conjecture 6.1. *Let Σ be a periodic hypersurface structure in \mathbb{R}^n , where $n > 2$. Then the spectrum of the corresponding Dirichlet-to-Neumann operator N has only a finite number of gaps.*

It is interesting to notice that the threshold between infinitely and finitely many gaps in the spectrum of N occurs between dimensions 2 and 3. Recall for comparison that for Schrödinger operators with periodic potentials the analogous threshold is between dimensions 1 and 2; see [Dahlberg and Trubowitz 1982; Karpeshina 1989b; 1989a; 1990a; 1990b; 1997; Skriganov 1979b; 1979a; 1984; 1985a; 1985b]. But there is no disagreement between these two cases, since we are dealing with Dirichlet-to-Neumann operators, which in 2D are essentially one-dimensional, and in 3D are two-dimensional.

We remind the reader that the operator N in 2D is responsible only for a part of the total spectrum of a photonic crystal. If this part of the spectrum

has few gaps, even less should be expected from the whole spectrum of the crystal.

We will prove now Conjecture 6.1 for the case of a cubic structure.

Theorem 6.2. *Let \mathbb{R}^3 be tiled with unit cubes and let Σ be the union of their surfaces. The spectrum of the corresponding Dirichlet-to-Neumann operator N has only a finite number of gaps. Moreover, there are no gaps in the spectrum for the values of the spectral parameter $D \geq 40\pi$.*

Proof. Let δ_Σ be the Dirac's delta function supported on Σ . Now we study the spectrum of the problem

$$-\Delta u = D\delta_\Sigma u.$$

Assuming that the edges of cubes are directed along the coordinate axes and taking into account that $\delta_\Sigma(x, y, z) = \delta_p(x) + \delta_p(y) + \delta_p(z)$, where δ_p is the sum of one-dimensional delta functions concentrated at the integers, we can separate variables: $u(x, y, z) = u_1(x)u_2(y)u_3(z)$, which leads to the system

$$\begin{cases} (-d^2/dx^2 - D\delta_p(x))u_1 = \mu_1 u_1, \\ (-d^2/dy^2 - D\delta_p(y))u_2 = \mu_2 u_2, \\ (-d^2/dz^2 - D\delta_p(z))u_3 = \mu_3 u_3, \\ \mu_1 + \mu_2 + \mu_3 = 0. \end{cases} \quad (6-1)$$

A real number D belongs to the spectrum if there is a triple of real numbers (μ_1, μ_2, μ_3) such that the system (6-1) has a non-trivial solution. One can see that either one or two among numbers μ_1, μ_2 , and μ_3 must be non-negative, and the remaining two or one must be non-positive. We will show that the case when there are two positive among these three numbers already guarantees the finiteness of the number of gaps, so we will consider only this case. Set $\mu_1 = -\lambda_1^2 \leq 0, \mu_2 = \lambda_2^2 \geq 0, \mu_3 = \lambda_3^2 \geq 0$, and $\lambda_1^2 = \lambda_2^2 + \lambda_3^2$. It is straightforward to check that non-trivial solvability of system (6-1) is equivalent to solvability with respect to D, λ_1 , and λ_2 of the system of inequalities

$$\begin{cases} \left| \cosh \lambda_1 - \frac{D}{2\lambda_1} \sinh \lambda_1 \right| \leq 1, & \left| \cos \lambda_2 - \frac{D}{2\lambda_2} \sin \lambda_2 \right| \leq 1, \\ \left| \cos \sqrt{\lambda_1^2 - \lambda_2^2} - \frac{D}{2\sqrt{\lambda_1^2 - \lambda_2^2}} \sin \sqrt{\lambda_1^2 - \lambda_2^2} \right| \leq 1. \end{cases} \quad (6-2)$$

Choose $\lambda_1 = D/2$ and $\lambda_2 = \pi m$ for an integer m . Then the system (6-2) reduces to a single inequality

$$\left| \cos \sqrt{(D/2)^2 - \pi^2 m^2} - \frac{1}{\sqrt{1 - \pi^2 m^2 (D/2)^{-2}}} \times \sin \sqrt{(D/2)^2 - \pi^2 m^2} \right| \leq 1. \quad (6-3)$$

Introduce numbers α (where $|\alpha| > m$) and $\beta > 1$ as follows:

$$D = 2\pi\alpha$$

and

$$\beta = (1 - \pi^2 m^2 (D/2)^{-2})^{-1/2} = (1 - m^2 \alpha^{-2})^{-1/2} > 1.$$

Let $\pi/4 < \gamma < \pi/2$ be an angle such that $\beta = \tan \gamma$. In fact, we will need $\gamma \leq \pi/3$, so we will try to satisfy the inequality

$$\beta \leq \sqrt{3}. \quad (6-4)$$

Now the inequality (6-3) becomes

$$\left| \cos \pi \sqrt{\alpha^2 - m^2} - \tan \gamma \sin \pi \sqrt{\alpha^2 - m^2} \right| \leq 1, \quad (6-5)$$

or

$$\left| \cos(\pi \sqrt{\alpha^2 - m^2} + \gamma) \right| \leq \cos \gamma,$$

which can be reduced to

$$n\pi + \gamma \leq \pi \sqrt{\alpha^2 - m^2} + \gamma \leq (n+1)\pi - \gamma$$

or

$$m^2 + n^2 \leq \alpha^2 \leq m^2 + (n+1 - 2\gamma/\pi)^2.$$

Since we plan to have $\gamma \leq \pi/3$, this inequality is satisfied if

$$m^2 + n^2 \leq \alpha^2 \leq m^2 + (n+1/3)^2. \quad (6-6)$$

Consider the family of segments

$$I_{n,m} = [m^2 + n^2, m^2 + (n+1/3)^2],$$

where m and n are integers. The statement of the theorem would follow if we were able to show that these segments cover a half-axis $[c, \infty)$. Notice that the segments $I_{n,m}$ are shifts (by m^2) of the segments $I_n = I_{n,0}$. The length of I_n is $|I_n| = 2n/3 + 1/9$. We first consider the sequence of segments $I_{n,m}$ for a fixed n and for $m = 0, 1, 2, \dots$. The segment $I_{n,m+1}$ is shifted with respect to $I_{n,m}$ by $2m+1$. Hence, until $2m+1$ stays less than $2n/3 + 1/9$, the sequence of segments $I_{n,m}$ for a fixed n covers a single segment

$$J_n = \bigcup \{ I_{n,m} : m \leq \frac{1}{3}n - \frac{4}{9} \}$$

without gaps. Now change the value of n in J_n . A sufficient non-emptiness condition for the intersection $J_n \cap J_{n+1}$ is

$$(n + 1/3)^2 + \lfloor n/3 - 4/9 \rfloor^2 \geq (n + 1)^2,$$

where $\lfloor a \rfloor$ denotes the integer part of a number a . It is not hard to check that this condition is satisfied for $n \geq 20$. We now need to check condition (6–4). It amounts to

$$m^2 \leq \frac{2}{3}\alpha^2.$$

Since we only use $m^2 \leq (n/3 - 4/9)^2$ and $\alpha^2 \geq n^2$, it is sufficient to check the inequality

$$(n/3 - 4/9)^2 \leq \frac{2}{3}n^2,$$

which is also satisfied in the range $n \geq 20$ that we chose. We can conclude that the intervals $I_{n,m}$ cover the whole half-axis $[40\pi, \infty)$, which due to the relation $D = 2\pi\alpha$ proves the theorem. \square

6A. The Square Structure

Remark 6.3. Our choice of the restriction $\gamma \leq \pi/3$ in the proof of the theorem was rather arbitrary. It certainly influenced our estimate of the upper bound for gaps in the spectrum. One could try to find the wisest choice of γ and hence to improve the estimate. There is, however, little hope that one can get the exact value of the threshold in this way. On the other hand, since our analytic estimate is quite reasonable, below it one can compute the spectrum numerically using the transcendental system (6–2). Figure 17 shows the result of the corresponding computation. The white horizontal axis in the middle of the picture is the spectral axis. Numerics shows that below 40π there are only three small gaps in the spectrum (three black segments on the spectral axis), the highest (and tiniest) of them ending at about $D = 17.83$. This, together with the statement of the theorem, shows that in fact there are no gaps anywhere beyond this value.

Remark 6.4. It is not hard to prove that the statement on finiteness of number of gaps for the cubic structure holds in any dimension $n > 2$. The proof is analogous to the one provided above.

7. CONCLUSIONS AND OPEN PROBLEMS

We summarize briefly the results of our analysis.

- The proposed algorithm works well for computing the spectra of waves localized in the dielectric regions of high contrast periodic 2D photonic band

gap structures. Here high contrast means small δ and large $\varepsilon\delta$.

- The spectra of many structures show asymptotically periodic behavior for large values of the spectral parameter. An analytic explanation of this phenomenon is provided.

- Disconnected structures have spectra that become practically discrete—that is, have very narrow bands for large values of the spectral parameter. This happens since disjoint parts of the structure essentially decouple at large frequencies. In the case of smooth disconnected structures an asymptotic formula for the location of the bands is developed in terms of the spectrum of the Laplace–Beltrami operator on one component of the structure.

- Many connected geometries (excluding, however, the rectangular one) support “almost localized” waves that produce high spikes in the density of states. These waves are mostly supported along some cycles or single edges of the structure. The existence of such waves apparently depends on geometry of joints. Symmetry arguments are provided that explain the existence of this effect for some geometries.

- Spectral gaps are rare and hard to achieve in dimensions higher than two. For instance, there is only a finite number of gaps for the cubic structure in dimensions three and higher.

Open Problems

- Prove an analog of the Bethe–Sommerfeld conjecture for the spectral problems of the photonic crystal theory, and in particular for the Dirichlet-to-Neumann operator on periodic surfaces.

- Prove absolute continuity of the spectra of the same problems. This problem boils down to showing the absence of the point spectrum. One has to be careful here, since our recent study shows that some differential operators on periodic graphs arising in mesoscopic physics do possess non-empty point spectrum. The conjecture, however, is probably true for the Dirichlet-to-Neumann operators.

- Explain the asymptotically periodic structure of spectra for more general classes of periodic graphs.

- Justify the almost discreteness of the spectra of Dirichlet-to-Neumann operators on non-smooth disconnected periodic graphs by elaborating the heuristic consideration of the beginning of Section 5B.

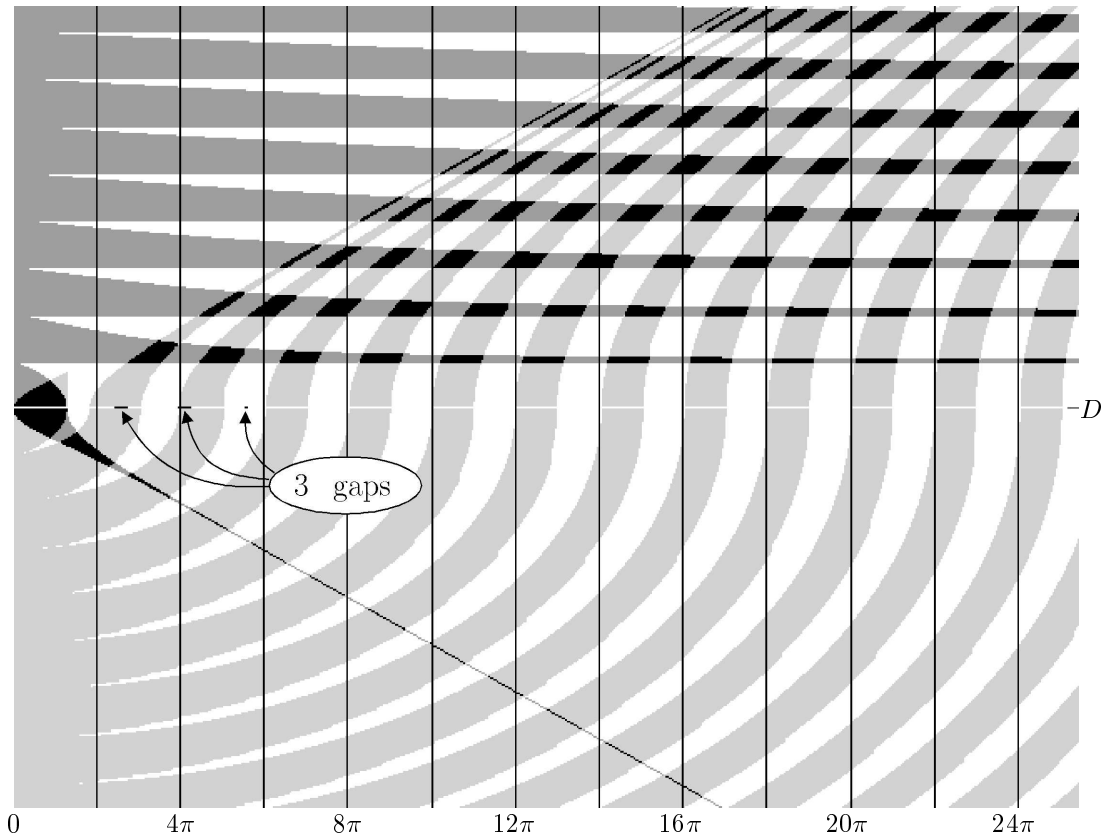


FIGURE 17. Spectrum of the 3D cubic structure.

- Introduce, when possible, an analog of the Laplace–Beltrami operator on a graph such that a version of Theorem 5.1 holds.

- Explain the phenomenon of the spikes of the density of states (“embedded eigenvalues”) in situations more general than the ones treated in Section 5C.

- Prove finiteness of the number of gaps for periodic 3D surface structures more general than the cubic one.

ACKNOWLEDGMENTS

The authors express their gratitude to Professors P. Exner, A. Figotin, A. Klein, and Dr. I. Ponomarev for helpful discussions. We are thankful to Professors V. Isakov, S. Molchanov, and Z. Sun for references to literature and to reviewers for important remarks.

REFERENCES

[Ashcroft and Mermin 1976] N. W. Ashcroft and N. D. Mermin, *Solid State Physics*, Holt, Rinehart and Winston, New York and London, 1976.

[Avron et al. 1994] J. E. Avron, P. Exner, and Y. Last, “Periodic Schrödinger operators with large gaps and Wannier–Stark ladders”, *Phys. Rev. Lett.* **72** (1994), 896–899.

[Bowden et al. 1993] C. M. Bowden et al., “Development and applications of materials exhibiting photonic band gaps”, *J. Opt. Soc. Amer. B* **10** (1993), 280–413. A collection of articles.

[Carlson 1997] R. Carlson, “Hill’s equation for a homogeneous tree”, *Electron. J. Differential Equations* **1997:23** (1997), 1–30.

[Carlson 1998] R. Carlson, “Adjoint and self-adjoint differential operators on graphs”, *Electron. J. Differential Equations* **1998:6** (1998), 1–10.

[Carlson 1999] R. Carlson, “Inverse eigenvalue problems on directed graphs”, *Trans. Amer. Math. Soc.* (1999). To appear.

[Dahlberg and Trubowitz 1982] B. Dahlberg and E. Trubowitz, “A remark on two dimensional potentials”, *Comment. Math. Helv.* **57** (1982), 130–134.

[Eastham 1973] M. S. P. Eastham, *The spectral theory of periodic differential equations*, Scottish Acad. Press, Edinburgh and London, 1973.

- [Edmunds and Evans 1987] D. E. Edmunds and W. D. Evans, *Spectral theory and differential operators*, Oxford Sci. Publ., Oxford, 1987.
- [Exner 1995] P. Exner, “Lattice Kronig–Penney models”, *Phys. Rev. Lett.* **74** (1995), 3503–3506.
- [Exner and Seba 1989] P. Exner and P. Seba, “Electrons in semiconductor microstructures: a challenge to operator theorists”, pp. 79–100 in *Schrödinger operators: standard and nonstandard* (Dubna, 1988), edited by P. Exner and P. Seba, World Scientific, Singapore and Teaneck, NJ, 1989.
- [Figotin 1994] A. Figotin, “Photonic pseudogaps in periodic dielectric structures”, *J. Stat. Phys.* **74**:1/2 (1994), 443–446.
- [Figotin and Godin 1997] A. Figotin and Y. Godin, “Computation of spectra of some 2D photonic crystals”, *J. Comput. Physics* **136** (1997), 585–598.
- [Figotin and Kuchment 1995] A. Figotin and P. Kuchment, “Band-gap structure of spectra of periodic and acoustic media, II: 2D Photonic crystals”, Technical Report 1995-1, Math. Dept., UNCC, 1995.
- [Figotin and Kuchment 1996a] A. Figotin and P. Kuchment, “Band-gap structure of spectra of periodic and acoustic media, I: Scalar model”, *SIAM J. Appl. Math.* **56**:1 (1996), 68–88.
- [Figotin and Kuchment 1996b] A. Figotin and P. Kuchment, “Band-gap structure of spectra of periodic and acoustic media, II: 2D photonic crystals”, *SIAM J. Appl. Math.* **56** (1996), 1561–1620. An abridged version of [Figotin and Kuchment 1995].
- [Figotin and Kuchment 1998a] A. Figotin and P. Kuchment, “2D photonic crystals with cubic structure: asymptotic analysis”, pp. 23–30 in *Wave propagation in complex media* (Minneapolis, 1994), edited by G. Papanicolaou, IMA Vol. in Math. and Appl. **96**, Springer, New York, 1998.
- [Figotin and Kuchment 1998b] A. Figotin and P. Kuchment, “Spectral properties of classical waves in high-contrast periodic media”, *SIAM J. Appl. Math.* **58**:2 (1998), 683–702.
- [Figotin and Kuchment – to appear] A. Figotin and P. Kuchment, “Asymptotic models of high contrast periodic photonic and acoustic media”. In preparation.
- [Freidlin and Wentzell 1993] M. I. Freidlin and A. D. Wentzell, “Diffusion processes on graphs and the averaging principle”, *Ann. Probab.* **21**:4 (1993), 2215–2245.
- [Glazman 1966] I. M. Glazman, *Direct methods of qualitative spectral analysis of singular differential operators*, Daniel Davey, Inc., New York, 1966. Translated from the Russian by the Israel Program for Scientific Translations, Jerusalem, 1965.
- [Joannopoulos et al. 1995] J. D. Joannopoulos, R. D. Meade, and J. N. Winn, *Photonic crystals: molding the flow of light*, Princeton Univ. Press, Princeton, 1995.
- [John 1991] S. John, “Localization of light”, *Phys. Today* **44**:5 (May 1991), 32–40.
- [Karpeshina 1989a] Y. Karpeshina, “Analytic perturbation theory for a periodic potential”, *Izv. Akad. Nauk SSSR, Ser. Math.* **52**:1 (1989), 45–65. In Russian; translated in *Math. USSR Izv.* **34** (1990).
- [Karpeshina 1989b] Y. Karpeshina, “Geometrical background for the perturbation theory of the polyharmonic operator with periodic potential”, pp. 251–276 in *Topological phases in quantum theory* (Dubna, 1988), edited by B. Markovski and S. I. Vinitzky, World Scientific, Singapore and Teaneck, NJ, 1989.
- [Karpeshina 1990a] Y. Karpeshina, “Perturbation theory for Schrödinger operator with a periodic potential”, pp. 131–145 in *Schrödinger operators, standard and non-standard* (Dubna, 1988), edited by P. Exner and P. Seba, World Scientific, Singapore and Teaneck, NJ, 1990.
- [Karpeshina 1990b] Y. Karpeshina, “Perturbation theory for the Schrödinger operator with a periodic potential”, *Trudy Mat. Inst. Steklov.* **188**:3 (1990), 88–116. In Russian; translated in *Proc. Steklov Inst. of Math.* **191** (1991), 109–145.
- [Karpeshina 1997] Y. Karpeshina, *Perturbation theory for the Schrödinger operator with a periodic potential*, Lecture Notes in Math. **1663**, Springer, 1997.
- [Kuchment 1982] P. Kuchment, “Floquet theory for partial differential equations”, *Russian Math. Surveys* **37**:4 (1982), 1–60.
- [Kuchment 1993] P. Kuchment, *Floquet theory for partial differential equations*, Birkhäuser, Boston and Basel, 1993.
- [Leung and Liu 1990] K. M. Leung and Y. F. Liu, “Full vector wave calculation of photonic band structures in face-centered-cubic dielectric media”, *Phys. Rev. Lett.* **65** (1990), 2646.
- [Maradudin and McGurn 1993] A. A. Maradudin and A. R. McGurn, “Photonic band gaps of a truncated, two-dimensional periodic dielectric media”, *J. Opt. Soc. Amer. B* **10** (1993), 307–313.
- [McCall et al. 1991] S. L. McCall, P. M. Platzman, R. Dalichaouch, D. Smith, and S. Schultz, “Microwave propagation in two-dimensional dielectric lattices”, *Phys. Rev. Lett.* **67**:17 (1991), 2017–2020.

- [Meade et al. 1992] R. D. Meade, K. D. Brommer, A. M. Rapper, and J. D. Joannopoulos, “Existence of photonic band gap in two dimensions”, *Appl. Phys. Lett.* **61** (1992), 495–497.
- [Plihal and Maradudin 1991] M. Plihal and A. A. Maradudin, “Photonic band structure of two-dimensional systems: The triangular lattice”, *Phys. Rev. B* **44** (1991), 8565–8571.
- [Ponomarev 1999] I. Ponomarev, “Separation of variables in the computation of spectra in 2D photonic crystals”, *SIAM J. Appl. Math.* (1999). To appear.
- [Reed and Simon 1978] M. Reed and B. Simon, *Methods of modern mathematical physics, IV: Analysis of operators*, Academic Press, 1978.
- [Rubinstein and Schatzman 1998] J. Rubinstein and M. Schatzman, “Asymptotics for thin superconducting rings”, *J. Math. Pures Appl.* (9) **77**:8 (1998), 801–820.
- [Schatzman 1996] M. Schatzman, “On the eigenvalues of the Laplace operator on a thin set with Neumann boundary conditions”, *Appl. Anal.* **61**:3-4 (1996), 293–306. Erratum in **62**:3–4 (1996), 405.
- [Shubin 1979] M. Shubin, “Spectral theory and the index of elliptic operators with almost periodic coefficients”, *Uspekhi Mat. Nauk* **34**:2 (1979), 95–135. In Russian; translation in *Russian Math. Surveys*.
- [Sigalas et al. 1993] M. Sigalas, C. M. Soukoulis, E. N. Economou, C. T. Chan, and K. M. Ho, “Photonic band gaps and defects in two dimensions: studies of the transmission coefficient”, *Phys. Rev. B* **48**:19 (1993), 14121–14126.
- [Skriganov 1979a] M. M. Skriganov, “On the Bethe–Sommerfeld conjecture”, *Soviet Math. Dokl.* **20** (1979), 89–90.
- [Skriganov 1979b] M. M. Skriganov, “Proof of the Bethe–Sommerfeld conjecture in dimension two”, *Sov. Math. Dokl.* **20** (1979), 956–959.
- [Skriganov 1984] M. M. Skriganov, “Proof of the Bethe–Sommerfeld conjecture in dimension three”, preprint P-6-84, LOMI, Leningrad, 1984. In Russian.
- [Skriganov 1985a] M. M. Skriganov, “Geometric and arithmetic methods in the spectral theory of multidimensional periodic operators”, *Proc. Steklov Inst. of Math.* **171** (1985), 1–117.
- [Skriganov 1985b] M. M. Skriganov, “The spectrum band structure of the three dimensional Schrödinger operator with periodic potential”, *Invent. Math.* **80** (1985), 107–121.
- [Soukoulis 1993] C. M. Soukoulis (editor), *Photonic Bands and Localization*, edited by C. M. Soukoulis, Plenum Press, New York, 1993.
- [Sylvester and Uhlmann 1988] J. Sylvester and G. Uhlmann, “Inverse boundary value problems at the boundary-continuous dependence”, *Comm. Pure Appl. Math.* **91** (1988), 197–219.
- [Villaneuve and Piché 1991] P. R. Villaneuve and M. Piché, “Photonic band gaps of transverse-electric models in two-dimensionally periodic media”, *J. Opt. Soc. America A* **8** (1991), 1296–1305.
- [Villaneuve and Piché 1994] P. R. Villaneuve and M. Piché, “Photonic band gaps in periodic dielectric structures”, *Prog. Quant. Electr.* **18** (1994), 153–200.
- [Zhang and Sathpathy 1990] Z. Zhang and S. Sathpathy, “Electromagnetic wave propagation in periodic structures: Bloch wave solution of Maxwell’s equations”, *Phys. Rev. Lett.* **65** (1990), 2650.

Peter Kuchment, Department of Mathematics and Statistics, Wichita State University, Wichita, KS 67260-0033
(kuchment@twsuvm.uc.twsu.edu, <http://www.math.twsu.edu/Faculty/Kuchment/>)

Leonid A. Kunyansky, Department of Applied Mathematics, California Institute of Technology, Pasadena, CA 91125
(leonk@ama.caltech.edu)